Development 136, 3767-3777 (2009) doi:10.1242/dev.033449

Conserved regulatory sequences in *Atoh7* mediate non-conserved regulatory responses in retina ontogenesis

Dorota Skowronska-Krawczyk[1,*,†,‡], Florence Chiodini[2,‡], Martin Ebeling[3], Christine Alliod[1], Adam Kundzewicz[1,2], Diogo Castro[4], Marc Ballivet[1], François Guillemot[4], Lidia Matter-Sadzinski[1,2] and Jean-Marc Matter[1,2,*]

The characterisation of interspecies differences in gene regulation is crucial to understanding the molecular basis of phenotypic diversity and evolution. The *atonal* homologue *Atoh7* participates in the ontogenesis of the vertebrate retina. Our study reveals how evolutionarily conserved, non-coding DNA sequences mediate both the conserved and the species-specific transcriptional features of the *Atoh7* gene. In the mouse and chick retina, species-related variations in the chromatin-binding profiles of bHLH transcription factors correlate with distinct features of the *Atoh7* promoters and underlie variations in the transcriptional rates of the *Atoh7* genes. The different expression kinetics of the *Atoh7* genes generate differences in the expression patterns of a set of genes that are regulated by Atoh7 in a dose-dependent manner, including those involved in neurite outgrowth and growth cone migration. In summary, we show how highly conserved regulatory elements are put to use in mediating non-conserved functions and creating interspecies neuronal diversity.

KEY WORDS: Ath5, Neurogenin 2, Trans-acting environment, Chicken, Mouse, Retinal ganglion cells

INTRODUCTION

The idea that vertebrate development is controlled by cis-regulatory elements is largely influenced by earlier work undertaken in invertebrates, such as *Drosophila* and sea urchin. These studies identified cis-regulatory elements that comprise target sites for large numbers of transcription factors that collectively instruct the regulatory networks of developmental genes (Davidson et al., 2002; Sandmann et al., 2007; Schroeder et al., 2004). As a first step towards deciphering such networks in vertebrates, a number of pair-wise and multiple-species whole-genome comparisons have been carried out to identify non-coding sequences conserved between highly divergent species (Birney et al., 2007).

That conserved non-coding elements have a role in the regulation of ontogenic events raises questions about whether they act similarly in distantly related animal species. It is of special interest to understand how variations in the interactions taking place at conserved non-coding elements may lead to interspecies cell diversity during ontogenesis of the nervous system.

Although the plan of the retina is well conserved across vertebrate evolution, there are considerable variations in cell type diversity and number, as well as in the organisation and properties of the tissue (Masland, 2001). Mammals typically have two distinct cones, whereas four cones persist in birds. Consequently, the postsynaptic wiring is expected to be more complex in birds and the far more elaborate dendritic arbors of chicken retinal ganglion cells (RGCs) compared with mouse RGCs might reflect such an increased complexity of signal processing (Kong et al., 2005; Naito and Chen, 2004).

A common feature of vertebrate retinogenesis is that RGCs differentiate first (Livesey and Cepko, 2001) and that the *atonal* homologue *Atoh7* gene (also known as *Math5* in the mouse, *Cath5* in chicken, and *Xath5* in *Xenopus*) is required for their production (Brown et al., 2002; Brown et al., 1998; Kanekar et al., 1997; Kay et al., 2001; Liu et al., 2001; Matter-Sadzinski et al., 2001). In zebrafish and mouse, inactivation of *Atoh7* results in a retina lacking most RGC types, including the small subset of RGCs that project to the suprachiasmatic nuclei and entrain circadian rhythms, whereas the other retinal cell types are produced in proportions that may differ from the wild type (Brown et al., 2001; Brzezinski et al., 2005; Kay et al., 2001; Le et al., 2006; Wang et al., 2001). During early retina development, Atoh7 is not exclusively expressed in the RGC lineage and hence may influence the production of other retinal cell types (Matter-Sadzinski et al., 2005; Yang et al., 2003).

Although the role of Atoh7 in the production of RGCs in the vertebrate retina is well established, it is unclear how this protein contributes to neuronal diversity across species. In particular, it is unclear whether variations result from species-specific properties of the Atoh7 protein (Brown et al., 1998; Sun et al., 2003) or whether they arise from differences in *Atoh7* gene regulation.

Multi-species alignments have identified several highly conserved regulatory elements within the non-coding sequence 5′ of the *Atoh7* gene (Hutcheson et al., 2005; Matter-Sadzinski et al., 2001; Matter-Sadzinski et al., 2005; Skowronska-Krawczyk et al., 2004). Whereas site occupancy and functional analyses have shown that the Ngn2 (Neurog2) and Atoh7 basic helix-loop-helix (bHLH) proteins are required for transcription of the chicken *Atoh7* gene (Hernandez et al., 2007; Matter-Sadzinski et al., 2001; Matter-Sadzinski et al., 2005; Skowronska-Krawczyk et al., 2004), the late onset of Ngn2 expression and the continued expression of the mutated *Atoh7* gene in *Math5*$^{-/-}$ mice have

[1]Department of Biochemistry, Sciences II, University of Geneva, 1211 Genève 4, Switzerland. [2]Department of Ophthalmology, School of Medicine, University of Geneva, 1211 Genève 4, Switzerland. [3]Bioinformatics, F. Hoffmann-La Roche, Basel 4070, Switzerland. [4]Division of Molecular Neurobiology, National Institute for Medical Research, The Ridgeway, Mill Hill, London NW7 1AA, UK.

*Authors for correspondence (dkrawczyk@ucsd.edu; Jean-Marc.Matter@unige.ch)
[†]Present address: University of California, San Diego, 9500 Gilman Drive, MC 0648, La Jolla, CA 92093-0648, USA
[‡]These authors contributed equally to this work

Accepted 10 September 2009

suggested that these factors are not involved in the regulation of *Atoh7* in mouse (Brown et al., 1998; Brown et al., 2001; Hutcheson et al., 2005; Wang et al., 2001).

The differences between mouse and chicken in the regulation of *Atoh7* are used in the present study to compare the function of evolutionarily conserved regulatory sequences that include several bHLH binding sites. In both the developing mouse and chick retina, Ngn2 protein was found to bind non-coding sequences 5′ of the *Atoh7* gene. This binding was exclusively detected in retina, suggesting that Ngn2 helps to establish the retina-specific expression of *Atoh7* in birds and mammals. Evolutionarily conserved regulatory elements were identified in the proximal and distal promoter regions of *Atoh7* and their in vivo occupancy by Ngn2 was found to be different in the mouse and chick retina. Species-related variations in the binding profiles correlated with distinct properties of the *Atoh7* promoters and appeared to underlie the different expression kinetics of the *Atoh7* gene in the respective retinas. High-level expression of Atoh7 in the chick retina activates a set of genes that are expressed in newborn RGCs and involved in neurite outgrowth and growth cone migration. In summary, we show how variations in the activation of highly conserved regulatory elements may facilitate interspecies neuronal diversity.

MATERIALS AND METHODS

Animals

Chick embryos from a White Leghorn strain were staged according to Hamburger and Hamilton (HH) (Hamburger and Hamilton, 1951). Mouse embryos were staged using the morning of the vaginal plug as embryonic day (E) 0.5. CD1 mice (Charles River) were used for electroporation experiments. *Ngn2* mutant lines in which a *GFP* cassette was knocked into the *Ngn2* locus were maintained as heterozygotes on a CD1 background (Seibt et al., 2003). The $Ngn2^{GFP/GFP}$ and wild-type control mice were littermates. Experimental procedures were carried out in accordance with Federal Swiss Veterinary Regulations.

Plasmids

For in situ hybridisation and dissociated cell in situ hybridisation (Matter-Sadzinski et al., 2001), ^{35}S-labelled antisense riboprobes were synthesized from linearised pBluescript derivatives using T7, T3 or SP6 RNA polymerase as appropriate. Mouse Ngn2 and Ash1, chicken Atoh7, human (h) ATOH7, STMN2 and PTN riboprobes encompassed the whole of the respective coding sequences. Primers used for cloning the targets are listed in Table 1. The pEMSV plasmid (Matter-Sadzinski et al., 2001) was used throughout to express the chicken *Atoh7* cDNAs in co-transfection and electroporation experiments. For transfection of P19 cells, mouse *Mash1* and *Ngn2* were cloned upstream of an IRES and an NLS-tagged GFP in the pCAGGS expression vector (Castro et al., 2006; Farah et al., 2000).

Chromatin immunoprecipitation (ChIP) assays

ChIP assays (primers are listed in Table 1) were performed essentially as described (Castro et al., 2006; Skowronska-Krawczyk et al., 2004) using mouse anti-Ngn2 (Heng et al., 2008), anti-Atoh7 (Abnova, Abcam), anti-Ash1 antibodies (Lo et al., 2002) and chicken anti-Atoh7 and anti-Ngn2 antibodies (Skowronska-Krawczyk et al., 2004). Immunoprecipitated DNA sequences were quantified by real-time PCR (Hernandez et al., 2007). For localisation of the binding sites of the chicken Atoh7 protein in the *Atoh7* promoter, dye-labelled DNA from immunoprecipitated chromatin was hybridised to a custom-designed microarray that encompassed a sequence extending ~2.2 kb upstream of the first coding ATG. This genomic region was tiled at 100 bp intervals using variable-length (65-75 bases) polynucleotides (NimbleGen Systems).

Electrophoretic mobility shift assays (EMSAs)

The preparation of protein extracts and EMSAs were performed as described (Hernandez et al., 2007).

Table 1. Primers used in this study

	Sequence (5′ to 3′)	
Gene	Forward	Reverse
Mouse ChIP		
Atoh7 proximal	GACGAAGGCAATGATGTCAG	CATCTCAGCACCTTCCTAC
Atoh7 distal	AGCCCAAAGAAAGCAGAC	TTCTGCGCTGGGAACAAC
Dll4	GGCCAGGATGAGGATATG	GGTCCTCAGCTGTATGGTAATG
Mouse RNA		
Atoh7	GGGCCAGGACAAGAAGC	CTAGGATGCGGGTGAGC
Ngn2	ACATCTGGAGCCGCGTAG	CCCAGCAGCATCAGTACC
Dll4	ACCACTTCGGACATTATGAG	CTCATGACAGCCAGAAAGAC
Stmn2	TGATCTGCTCCTGCTTCTAC	CGCTTGTTGATCTGCTTCAC
Ptn	AGCGATACCTGGAGTCTG	CGTTGCTGCTGATATTGC
Snap25	GATCAGCGGACAGCATCCTC	CTTCGGCCATGGTACTGGTG
Robo2	TTGTGTTGCAAGGAACTATC	CCAGCTGCGACTACCACATC
Gapdh	TCAACAGCAACTCCCACTCTTCCA	ACCCTGTTGCTGTAGCCGTATTCA
Chicken ChIP		
Atoh7 proximal	ATGTTCGGGTTTTACTGTTGCTTC	GAAGACATAACTTGGTAACAGAAATC
Atoh7 distal	TAACAGCCTACGTTCAACATC	GCAGAAGCAATGACAATGAAATGAG
Stmn2	CACAACTTCCCAGTGGCTATC	TACATCTGGAGCTGCCTATGC
Snap25	GGGCATAAGCTTGACCTTGG	CGCAGCTGAATAGTCAGGAG
Chicken RNA		
Atoh7	GAGAATGGATTAACCTTCACTGTGAAC	GCTGTGCATAAGGATCACTGTCTG
Mouse/chicken 18S	CTTAGAGGGACAAGTGGCG	GCTGAGCCAGTCAGTGTA
Stmn2	CCTGAACCTCGCAACA	AGTTCGTGGTGCTTCC
Ptn	CTCTCCTGGCACTTGTCTTC	CAGACACTCCACTGCCATTC
Robo2	GACAGGGAAGAGCGGATCAG	TGTTGGTTCCAACGCAAGTG
Snap25	TATGCGCAATGAGTTGGAAG	TCAACAAGTTGCAGCATTCG
Gapdh	ATGATCCCTTCATCGATCTG	ATCACAAGTTTCCCGTTCTC

Atoh7 promoter constructions

Wild-type and mutated upstream sequences that were 2.22 kb in length and bounded by *Eco*RI and *Bst*XI restriction sites were subcloned in the proper orientation at appropriate sites in the vectors p00-CAT, p00-lac, pEGFP (Hernandez et al., 2007) and pDsRed2-N1 (Clontech). Mutagenesis was performed as described (Hernandez et al., 2007).

Immunopanning, cell culture, transfection, *CAT* and *lacZ* expression assays

For Affymetrix analysis, two independent immunopanning experiments of RGCs were performed as described (Skowronska-Krawczyk et al., 2004). Neuroretina tissues were dissected from HH22-30 embryos and dissociated retinal cells were prepared and transfected with *CAT* or *lacZ* reporter genes as described (Matter-Sadzinski et al., 2005). P19 cells were transfected as described (Castro et al., 2006).

Nascent transcript isolation

Nascent RNAs were isolated from HH27-37 retinas as described (Wuarin and Schibler, 1994).

mRNA quantification

RNA extraction, cDNA synthesis and real-time PCR were performed as described (Skowronska-Krawczyk et al., 2005). RNA samples were DNase I treated and all RT-PCR reactions were accompanied by RT(–) controls. All primers listed in Table 1 were tested for efficiency. *Gapdh* mRNA was used for normalisation. The numbers of RNA molecules per cell volume were quantified as follows. Mouse and chicken primers were used to generate reference PCR products. The number of reference products was determined using PicoGreen (Molecular Probes) quantification and their molecular masses. The number of isolated *Atoh7* mRNA molecules was calculated by comparison with a standard curve generated by serial dilutions of the reference PCR products.

Microarray analysis

The complete microarray dataset has been deposited in the public data repository of the European Bioinformatics Institute (ArrayExpress) with accession number E-TABM-417.

Electroporation of genetic material and confocal microscopy

Retina electroporation and confocal microscopy were performed as described (Hernandez et al., 2007; Matter-Sadzinski et al., 2005). For the E14.5 mouse ex vivo retina, electroporation consisted of five 30 V/cm pulses of 100 millisecond duration spaced 1 second apart.

RESULTS

Ngn2 regulates *Atoh7* expression in the embryonic mouse retina

In the developing chick retina, expression of Ngn2 and Atoh7 coincides (Matter-Sadzinski et al., 2001; Matter-Sadzinski et al., 2005), whereas in mouse a 48-hour lag period is reported to occur between the onset of Atoh7 (at E11.5) and Ngn2 (at E13.5) expression in the developing retina, suggesting that the mouse Ngn2 protein cannot be involved in the early activation of the *Atoh7* (Brown et al., 1998). Because significant differences in the expression patterns of Atoh7 and Ngn2 might underlie significant species-specific variations in retinogenesis, we have re-examined the expression of Atoh7, Ngn2 and Ash1 (Mash1, Ascl1) in the early mouse retina. At E11.5, *Atoh7* and *Ngn2* transcripts accumulated in overlapping domains that encompassed a more restricted *Ash1* expression region (Fig. 1A,B; see Fig. S1A,B in the supplementary material), indicating that the expression onsets of these genes coincide in the mouse retina. The early accumulation of *Ngn2* transcripts was confirmed by quantitative (q) PCR at E12.5 (Fig. 1D). However, the low level of *Ngn2* mRNA in the developing mouse retina contrasted with the robust expression of Ngn2 seen at the peak of Atoh7 expression in the chick retina (Matter-Sadzinski et al., 2001).

This finding prompted us to determine whether the Ngn2 protein was involved in the transcriptional activation of the mouse *Atoh7* gene. Comparing the accumulation of *Atoh7* transcripts in the retinas of wild-type and $Ngn2^{GFP/GFP}$ mice, we found that in situ

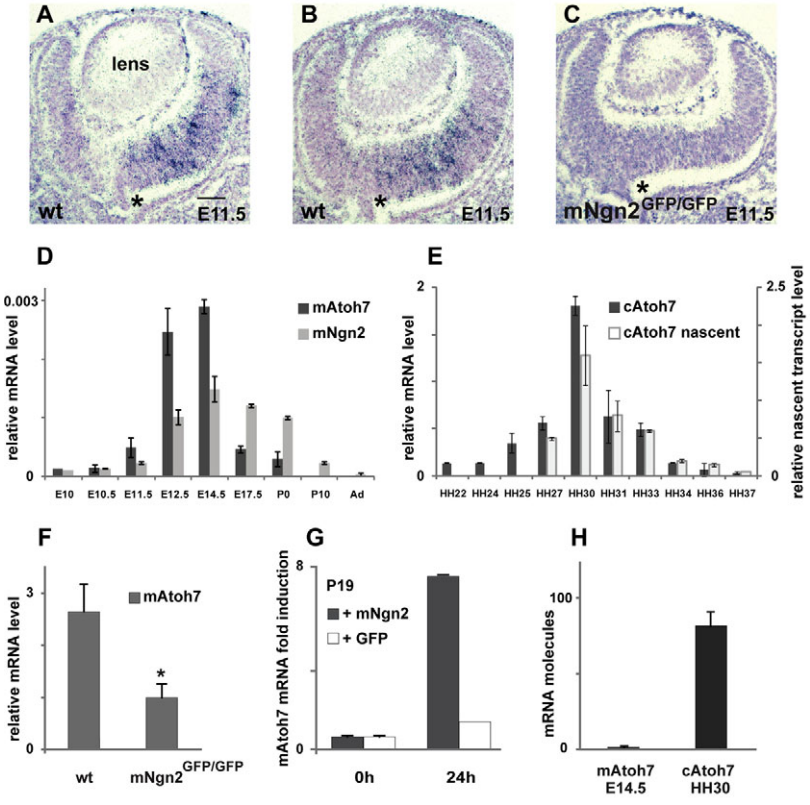

Fig. 1. Expression of Ngn2 and Atoh7 in mouse and chick retina. (**A-C**) At E11.5, mouse (m) *Ngn2* (A) and *Atoh7* (B) transcripts accumulate in discrete and overlapping domains in the wild-type (wt) mouse retina. There is very little accumulation of *Atoh7* transcripts in the $Ngn2^{GFP/GFP}$ retina (C). Dorsal is to the right. Asterisk marks the optic nerve. Scale bar: 40 μm. (**D**) Transcript levels during embryonic and postnatal mouse retina development. (**E**) Total and nascent transcript levels of chick (c) *Atoh7* during chick retina development. (**F**) qPCR analysis of *Atoh7* expression in wild-type and $Ngn2^{GFP/GFP}$ E12.5 mouse retina (*, $P<0.003$). (**G**) The mouse Ngn2 protein induces expression of the endogenous *Atoh7* gene in the P19 cell line. (**H**) Average numbers of *Atoh7* mRNA molecules per cell in E14.5 mouse and HH30 chick retinas.

DEVELOPMENT

hybridisation at E11.5 and qPCR analysis at E12.5 both revealed a much decreased level of *Atoh7* transcript in the retina of *Ngn2*$^{GFP/GFP}$ mice (Fig. 1C,F), suggesting that Ngn2 might contribute to the activation of *Atoh7* expression in the mouse retina. Likewise, we found that the expression of Atoh7 was activated by the misexpression of Ngn2 in the mouse P19 cell line (Fig. 1G). In agreement with our data, Trimarchi et al. have reported the co-expression of Ngn2 and Atoh7 in mouse retinal progenitors (Trimarchi et al., 2008).

The mouse and chicken Ngn2 proteins display different chromatin-binding profiles

In a first step towards the identification of regulatory sequences that could control transcription of the mouse *Atoh7* gene, we compared the relevant gene sequences of several vertebrate species (see Fig. S2 in the supplementary material). We detected three regions of high conservation, namely the coding sequence (CDS), a proximal and a distal upstream region. The coding region of *Atoh7* coincides with a strong conservation peak. Upstream of the transcribed region, the proximal conserved sequence extends over ~250 bp and harbours a predicted TATA box and two E-boxes (E1 and E2) in all species analysed. The proximal region also contains another well-conserved E-box (E4) in all species except *Xenopus*. Further upstream, the distal conserved region contains two predicted E-boxes (E8 and E9). This distal element is located within 2 kb upstream of the CDS, except in *Xenopus tropicalis*, where it is found 5 kb upstream of the CDS. Electrophoretic mobility shift assays (EMSAs) using proteins isolated from Atoh7-expressing cells revealed that Atoh7 binds to a DNA sequence encompassing E8 and E9 through its basic domain (see Fig. S3 in the supplementary material).

To test whether Ngn2 binds to any of the conserved regions within the regulatory sequences of the mouse *Atoh7* gene (Fig. 2A), we performed chromatin immunoprecipitation (ChIP) on chromatin isolated from E14.5 and adult mouse retinas. Primers were designed to discriminate between binding to the proximal region encompassing the E-boxes E1, E2 and E4, and binding to the distal region encompassing E-boxes E8 and E9. We found that Ngn2 bound the distal, but not the proximal, region during mouse embryonic development, whereas no binding of Ngn2 was detected in chromatin isolated from adult retina (Fig. 2B). Although Ngn2 is expressed in the E14.5 mouse telencephalon (Fode et al., 2000) (our unpublished data), it bound neither the distal nor the proximal region in this tissue (Fig. 2B). However, positive control ChIP experiments indicated that Ngn2 was bound to the *Delta1* (*Dll1*) promoter in chromatin derived from E14.5 telencephalon (Fig. 2B) (Castro et al., 2006), and in *Ngn2*-transfected murine P19 cells the mouse Ngn2 protein bound both the proximal and distal promoter regions of *Atoh7* (Fig. 2C). The lack of binding of Ngn2 to the proximal sequence in mouse retina contrasts with the strong binding of the chicken orthologue to the corresponding region in chicken *Atoh7* (Fig. 2D), whereas binding to the distal region is much lower (Fig. 2D). Conversely, chicken Atoh7 has a higher affinity for the distal than for the proximal region (Fig. 2E). Although Ngn2 is expressed in the developing chick optic tectum (Matter-Sadzinski et al., 2001), its binding to the promoter regions is at background level in this tissue (Fig. 2D) (Skowronska-Krawczyk et al., 2004).

ChIP assays using anti-mouse Atoh7 polyclonal and monoclonal antibodies from various sources did not show binding to the proximal or distal regions in the mouse retina (not shown). However, because no direct Atoh7 target gene has yet been identified, the experiment remains inconclusive for lack of a positive control. By contrast, targets for mouse Ash1 were identified in the telencephalon (Castro et al., 2006) and a ChIP assay enabled us to identify an Ash1-bound target in the E14.5 mouse retina (see Fig. S1C-E in the supplementary material). Under the same conditions, there was no

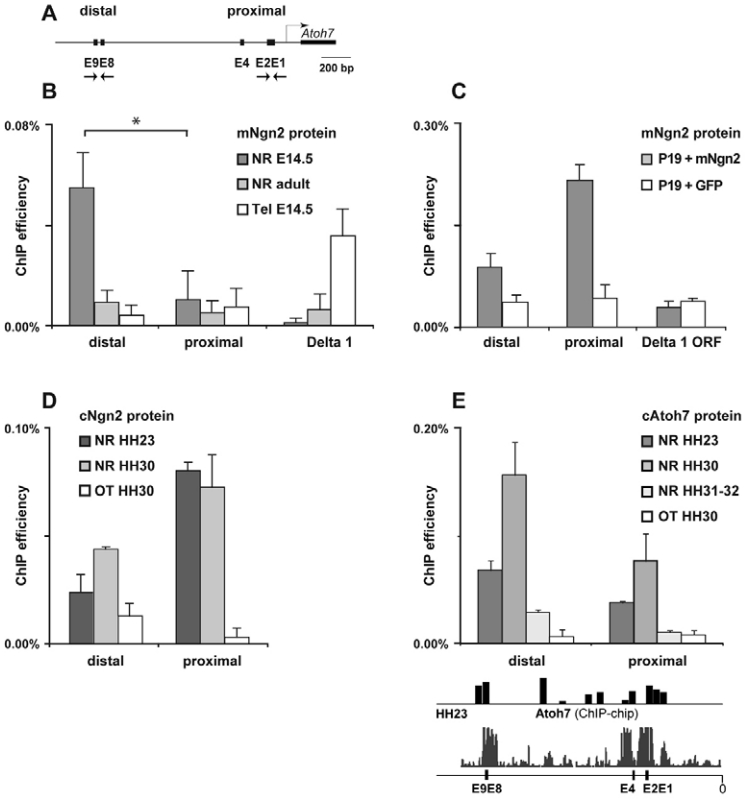

Fig. 2. In vivo occupancy of the distal and proximal promoter regions of the *Atoh7* gene by the mouse and chicken Ngn2 and Atoh7 proteins. (**A**) The proximal and distal upstream regions of the *Atoh7* gene. Locations of the E-boxes are shown and arrows mark the primers used for amplification (not to scale). (**B-E**) Antibodies directed against mouse Ngn2 (B,C), and chick Ngn2 (D) and Atoh7 (E) were used to immunoprecipitate cross-linked chromatin fragments prepared from E14.5 mouse retina, adult mouse retina, E14.5 mouse telencephalon (B), the P19 cell line (C), HH23, HH30, HH31-32 chick retina and HH30 chick optic tectum (D,E). Immunoprecipitates were analysed by qPCR for the abundance of proximal and distal mouse (B,C) and chicken (D,E) *Atoh7* regulatory sequences, *Delta1* regulatory sequences (B) and *Delta1* ORF (C) (*, $P<0.001$). The lower part of E illustrates the binding sites of the Atoh7 protein in HH23 chick retina. A ~2.2 kb sequence was tiled at 100 bp intervals. Alignments between probe coordinates and E-box positions were detected in three independent ChIP-chip experiments.

DEVELOPMENT

binding of Ash1 to the proximal or distal *Atoh7* promoter regions (data not shown), suggesting that Ash1 is not directly involved in the regulation of *Atoh7* in mouse.

Transcription of *Atoh7* obeys different kinetics in the mouse and chick retina

Having ascertained that Ngn2 is implicated in regulating *Atoh7* expression in both the mouse and chick retina, we asked whether the different occupancy patterns of the *Atoh7* promoters by Ngn2 lead to differences in the expression patterns of mouse and chick *Atoh7*. RNA isolated from mouse and chick retinas at different stages of development was reverse transcribed and quantified by qPCR (Fig. 1D,E).

In agreement with northern blot analysis (Matter-Sadzinski et al., 2001), the level of chick *Atoh7* mRNA increased ~10-fold between stages HH22 and HH30. To determine whether the rate of transcription of *Atoh7* increased during this period, we measured the accumulation of nascent *Atoh7* RNAs in nuclei isolated at different stages of chick development (Fig. 1E). The correlation between nascent transcripts and mRNA indicates that the transient upregulation of *Atoh7* is regulated at the transcriptional level. Beginning at HH31, transcription of *Atoh7* was downregulated (Fig. 1E) and the binding of Atoh7 to the distal and proximal regions decreased to a low level (Fig. 2E). Transcription of *Atoh7* peaked when the expression domain of Atoh7 had expanded to the periphery of the chick retina, the stage at which the majority of chicken RGCs are being generated.

In the mouse retina, peripheral expansion of the Atoh7 expression domain takes place between E11.5 and E14.5 (Brown et al., 1998) (our unpublished data). Although the level of mouse *Atoh7* mRNA peaked at ~E14.5, it was low when compared with the level of the control *Gapdh* mRNA (Fig. 1D).

By measuring the ratio between the amount of *Atoh7* mRNA and total DNA (compensating for genome size), we calculated that a mouse and a chick retinal cell contain, respectively, 1.5±0.5 and 81±9 *Atoh7* mRNA molecules. Cell volumes were estimated by measuring the ratio between the amount of 18S rRNA and total DNA (Schmidt and Schibler, 1995). We found that mouse retinal cells were on average ~2.5 times smaller at E14.5 than chick retinal cells at HH30. It follows that the concentration of *Atoh7* mRNA molecules is on average 15-40 times lower in mouse than in chick retinal cells (Fig. 1H). These values are averaged over whole retinas and we do not exclude the possibility that *Atoh7* is expressed at high levels in small subsets of cells. However, this possibility seems unlikely, given that similar proportions of Atoh7-expressing progenitors are detected in E16.5 mouse (Trimarchi et al., 2008) and HH23-30 chick (Skowronska-Krawczyk et al., 2004) retina.

The distal and proximal promoter regions cooperate to regulate *Atoh7* expression in the chick retina

In the chick retina, Ngn2 and Atoh7 bind the proximal *Atoh7* promoter. This ~0.9 kb sequence contains evolutionarily conserved regulatory elements that are sufficient to recapitulate the features of endogenous Atoh7 expression (Hernandez et al., 2007a; Matter-Sadzinski et al., 2005). However, whereas at HH22-23 ~25% of retinal progenitor cells accumulate *Atoh7* transcripts (Skowronska-Krawczyk et al., 2004), the activity of the electroporated proximal region could only be detected in a small fraction of these cells (Matter-Sadzinski et al., 2005). To determine whether the distal promoter region contributes to *Atoh7* promoter activity, a ~2.2 kb sequence that encompasses both the proximal and distal regions was fused to the *GFP* gene, the construct was electroporated into HH22-23 chick retina together with a CMV promoter/RFP control plasmid, and fluorescent cells were detected 24 hours later. Similar densities of RFP^+ cells were detected in the central and peripheral retina. By contrast, and congruent with the specific Atoh7 expression pattern (Matter-Sadzinski et al., 2005), GFP^+ cells accumulated in the central retina at a density corresponding to ~30% of the electroporated cells, whereas only a few scattered GFP^+ cells were detected at the periphery (Fig. 3A inset, and data not shown). The large increase in the proportion of cells that displayed promoter activity when using the ~2.2 kb sequence suggested that the distal sequences contribute to strengthen the promoter.

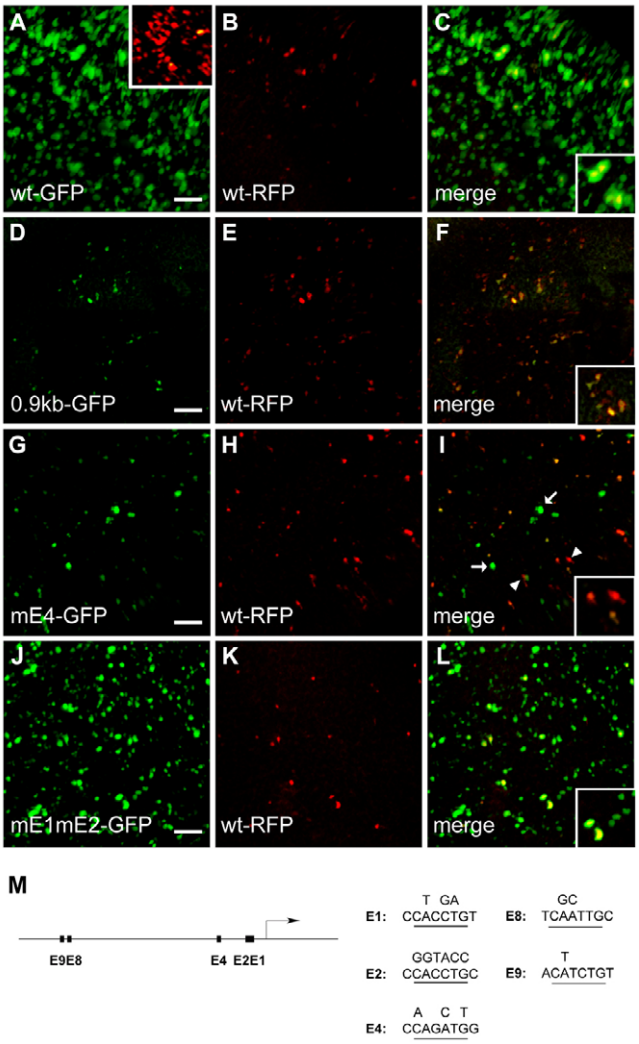

Fig. 3. The distal and proximal *Atoh7* promoter regions cooperate in the chick retina. (**A-L**) HH22-23 chick retinas were electroporated with plasmids as follows: $wt_{2.2kb}$/RFP plus $wt_{2.2kb}$/GFP (A-C) or $wt_{0.9kb}$/GFP (D-F) or $mE4_{2.2kb}$/GFP (G-I) or mE1mE2/GFP (J-L). (A, inset) Peripheral HH22-23 retina electroporated with $wt_{2.2kb}$/GFP and CMV promoter/RFP reporter plasmids. (C,F,I,L, insets) Magnifications of double-labelled cells. In I, arrowheads indicate cells expressing the wild-type but not the mutant promoter, whereas arrows indicate cells expressing the mutant but not the wild-type promoter. Scale bars: 50 μm. (**M**) E1, E2, E4, E8, E9 are the conserved E-boxes and mE1, mE2, mE4, mE8 and mE9 are the corresponding mutated E-boxes. The base changes introduced to mutate the underlined canonical E-box sites are shown.

To discriminate high versus low promoter activity in Atoh7-expressing cells, we used two different fluorescent proteins, one of which (RFP) has a lower quantum efficiency than the other (GFP). When $wt_{2.2kb}$/RFP and $wt_{2.2kb}$/GFP plasmids were electroporated into HH22-23 retina, ~95% of the RFP$^+$ cells co-expressed GFP and only ~20% of the abundant GFP$^+$ cells were double labelled (Fig. 3A-C, Fig. 4J). These might correspond to cells that have already upregulated *Atoh7*. Consistent with this idea, ~95% of GFP$^+$ cells co-expressed RFP when $wt_{0.9kb}$/GFP and $wt_{2.2kb}$/RFP plasmids were electroporated into HH22-23 retina (Fig. 3D-F, Fig. 4J). Moreover, ~70% of GFP$^+$ cells co-expressed RFP when $wt_{2.2kb}$/GFP and $wt_{2.2kb}$/RFP plasmids were electroporated into HH28 retina (see Fig. S4 in the supplementary material). The increase in the number and fluorescence intensity of the RFP$^+$ cells is consistent with the increased transcription rate of the *Atoh7* gene at this stage (Fig. 1E). To quantify the promoter strengths of the 0.9 kb and 2.2 kb sequences, the $wt_{2.2kb}$/CAT and the $wt_{0.9kb}$/CAT plasmids were transfected in HH22-23 and HH29-30 retinal cells and CAT activity was measured 24 hours later (Fig. 4K). Both sequences displayed upregulated activity at HH29-30 and the activity of the 2.2 kb sequence was consistently stronger than that of the 0.9 kb sequence at both stages. To confirm the specificity of the 2.2 kb sequence, a $wt_{2.2kb}$/lacZ plasmid was electroporated into HH28 retina and *lacZ*-expressing cells were detected 24 hours later. Dissociated cell in situ hybridisation revealed that ~92% of the *lacZ*-expressing cells accumulated *Atoh7* transcripts (see Fig. S8A,B,E in the supplementary material). In summary, we conclude that the distal region enhances *Atoh7* promoter activity along the pathway leading to the conversion of proliferating progenitors into RGCs.

The distal sequence encompasses the E-boxes E8 and E9 (see Fig. S2 in the supplementary material). To determine whether these conserved elements mediate the activity of the distal region, HH22-23 retinas were electroporated with mutant $mE8_{2.2kb}$, $mE9_{2.2kb}$ or $mE8mE9_{2.2kb}$/GFP plasmids plus a $wt_{2.2kb}$/RFP reporter plasmid. Whereas the $mE8_{2.2kb}$ and wild-type promoters displayed similar activities (Fig. 4A-C,J), both the number and fluorescence intensity of the GFP$^+$ cells were much decreased in the E9 and E8 E9 mutants (Fig. 4D-I,J). The activities of the mutant and wild-type promoters co-localised (Fig. 4C,F,I), indicating that E8 and E9 do not control promoter specificity. Since the distal region binds chick Atoh7, we tested whether this protein mediates the positive effect displayed by E9. HH28 retinas were electroporated with $mE8_{2.2kb}$, $mE9_{2.2kb}$ or $wt_{2.2kb}$/GFP plasmids plus a $wt_{2.2kb}$/RFP plasmid and an Atoh7 expression vector (see Fig. S5 in the supplementary material). Whereas numerous, intensely fluorescent GFP$^+$ and RFP$^+$ cells were detected with the wild-type and mE8 promoters (see Fig. S5A,B,D,E in the supplementary material), both the number and fluorescence intensity of the GFP$^+$ cells were decreased when E9 was mutated (see Fig. S5C,G in the supplementary material), confirming that Atoh7 can mediate a positive feedback via E9. To quantify this effect, $wt_{2.2kb}$ or $wt_{0.9kb}$/CAT plasmids plus an Atoh7 expression vector were transfected into HH29-30 retinal cells (Fig. 4K). Overexpression of Atoh7 enhanced the promoter activity of both the short and the long fragments, the higher activity of the long fragment probably reflecting the contribution of E9 to the positive feedback exerted by Atoh7.

To determine whether the distal region requires the conserved proximal regulatory elements for promoter activity, $mE4_{2.2kb}$, $mE1mE2_{2.2kb}$ or $mE1mE2mE4_{2.2kb}$/GFP plasmids plus a $wt_{2.2kb}$/RFP plasmid were electroporated into HH22-23 retina. Consistent with the antagonistic activities mediated by E1 and E2 (Hernandez et al., 2007), the net activity of the mE1mE2 promoter was similar to that of the wild-type promoter (Fig. 3J-L, Fig. 4J). By contrast, mutation of E4 led to a strong decrease in the size of the GFP$^+$ cell population (Fig. 3G-I, Fig. 4J). Moreover, a significant proportion of the rare GFP$^+$ cells did not co-express RFP and a fraction of RFP$^+$ cells was GFP$^-$ (Fig. 3I), indicating that E4 contributes to both the strength and the specificity of the *Atoh7* promoter.

Very rarely, GFP$^+$ cells were detected when E1, E2 and E4 were mutated (Fig. 4J). To determine whether the activation mediated by Atoh7 requires cooperation between E9 and the proximal E-boxes, HH22-23 and HH28-29 retinas were electroporated with a $mE1mE2mE4_{2.2kb}$/GFP plasmid, a $wt_{2.2kb}$/RFP plasmid and an Atoh7 expression vector. Despite the overexpression of Atoh7, the

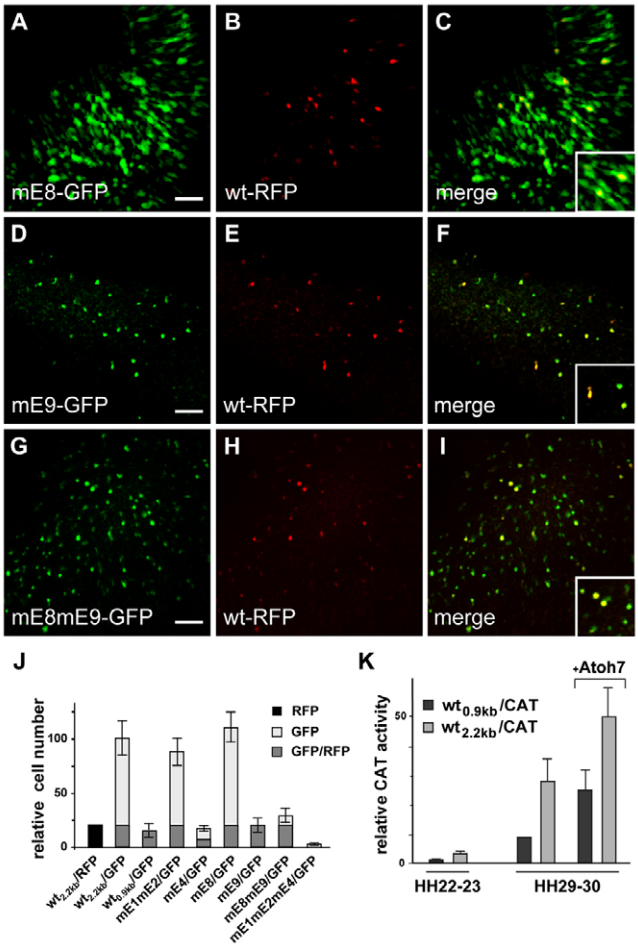

Fig. 4. In chick, the activity of the distal promoter region is mediated through E9. (**A-I**) HH22-23 chick retinas were electroporated with plasmids as follows: $wt_{2.2kb}$/RFP plus $mE8_{2.2kb}$/GFP (A-C) or $mE9_{2.2kb}$/GFP (D-F) or $mE8mE9_{2.2kb}$/GFP (G-I). (C,F,I, insets) Magnifications of double-labelled cells. Scale bars: 50 μm. (**J**) Cell number obtained with the $wt_{2.2kb}$/RFP plasmid is set at 20 and cell numbers obtained with the wild-type and mutant promoter/GFP plasmids are given relative to this value. Data are presented as the mean ± s.d.; at least five electroporated retinas were analysed per condition. (**K**) $wt_{2.2kb}$/CAT and $wt_{0.9kb}$/CAT plasmids were transfected into retinal cells isolated at HH22-23 and HH29-30. The CAT activity obtained upon transfection with the $wt_{0.9kb}$/CAT reporter plasmid at HH29-30 is set arbitrarily at 10 and activities of the mutants are given relative to this value. Relative promoter activities are shown as the mean ± s.d. of at least three independent experiments.

DEVELOPMENT

density of GFP$^+$ cells remained very low (see Fig. S6 in the supplementary material), suggesting that E9 requires the proximal E-boxes to mediate the effect of Atoh7.

Dominant activity of the distal region of *Atoh7* in the mouse retina

The fact that the bHLH binding profiles and the transcriptional rates of the *Atoh7* gene are different between mouse and chicken raises questions about the role of the conserved elements in the two species. To determine whether the observed interspecies differences result from sequence variations, we compared the promoter activities of the mouse 2.3 kb and chicken 2.2 kb sequences (see Fig. S2C in the supplementary material) in the context of the two types of retina. When pG1M5-2.3kb (mouse) (Hutcheson et al., 2005) and $wt_{2.2kb}$/RFP (chicken) plasmids were electroporated into E14.5 mouse ex vivo retina and into HH22-23 and HH28 chick ex vivo retinas, ~95% of the RFP$^+$ cells co-expressed GFP (Fig. 5P,R; see Fig. S7 in the supplementary material). In mouse retina, the two sequences displayed the same promoter activity (Fig. 5D,P-R). In chick retina, the promoter activity of the mouse sequence was upregulated between HH22-23 and HH28, as expected if responding to Atoh7 (see Fig. S7 in the supplementary material). When tested in the same species, the chicken and mouse sequences displayed very similar promoter properties, suggesting that the differences observed in the expression of the mouse and chicken *Atoh7* genes are mediated by conserved elements in response to different cellular contexts. Similarly, the promoter activity of the mouse 2.3 kb sequence is restricted to the *Xenopus* ciliary marginal zone where expression of *Xenopus Atoh7* takes place (Hutcheson et al., 2005).

To test whether interspecies variations result from the species-specific use of conserved elements, we looked at their activity in mouse. The $wt_{2.2kb}$, $mE1mE2_{2.2kb}$, $mE4_{2.2kb}$, $mE8_{2.2kb}$, $mE9_{2.2kb}$ or $mE8mE9_{2.2kb}$/GFP plasmids were electroporated into E14.5 mouse retina together with a $wt_{2.2kb}$/RFP or a CMV/RFP plasmid (Fig. 5). Consistent with the properties of the chicken 2.2 kb sequence in mouse, the wild-type and CMV promoters were active in distinct cell populations (Fig. 5A). Surprisingly, mutation of E9 was sufficient to inactivate the promoter (Fig. 5B,R). The few and faint GFP$^+$ cells observed did not co-express RFP when the retinas were co-electroporated with $mE9_{2.2kb}$/GFP and $wt_{2.2kb}$/RFP plasmids (Fig. 5G-I,R). This loss of specificity was also detected when both E8 and E9 were mutated (Fig. 5C,J-L,R). In the mouse context, E9 might therefore control both the specificity and the strength of the *Atoh7* promoter. The role of the proximal elements is unclear in this species: mutation of either E4 or E1 E2 had no effect on promoter activity (Fig. 5M-O,R). Thus, in contrast to its central role in the chick retina, E4 mediated neither the specificity nor the strength of the promoter in the mouse retina.

A set of genes associated with neurite outgrowth is regulated by Atoh7 in a dose-dependent manner

Atoh7 expression is strongly upregulated in the chick retina at the time RGCs are produced, whereas it remains at a low level throughout mouse retina development. This prominent difference in the kinetics of Atoh7 expression suggests that some, but not all, species require upregulation of Atoh7 in order to produce RGCs. To test this notion, we asked whether a precocious increase in the level of Atoh7 would activate genes involved in a chick-specific RGC developmental programme. We compared the transcriptome of HH22-23 retinas in which we overexpressed Atoh7 to that of controls expressing Atoh7 at a low level. To avoid stage- and sex-related heterogeneity, the experiment was conducted on individual embryos. The tested eye was electroporated with an Atoh7 expression vector and a CMV promoter/GFP reporter plasmid, while the contralateral control eye was electroporated with the reporter plasmid only. Retinal RNA was isolated 24 hours later and expression of the nicotinic acetylcholine receptor beta 3 (β*3nAChR*) gene, an established target of Atoh7, was assessed by qPCR (Skowronska-Krawczyk et al., 2005). The retinal RNAs from embryos in which the β*3nAChR* expression level was at least

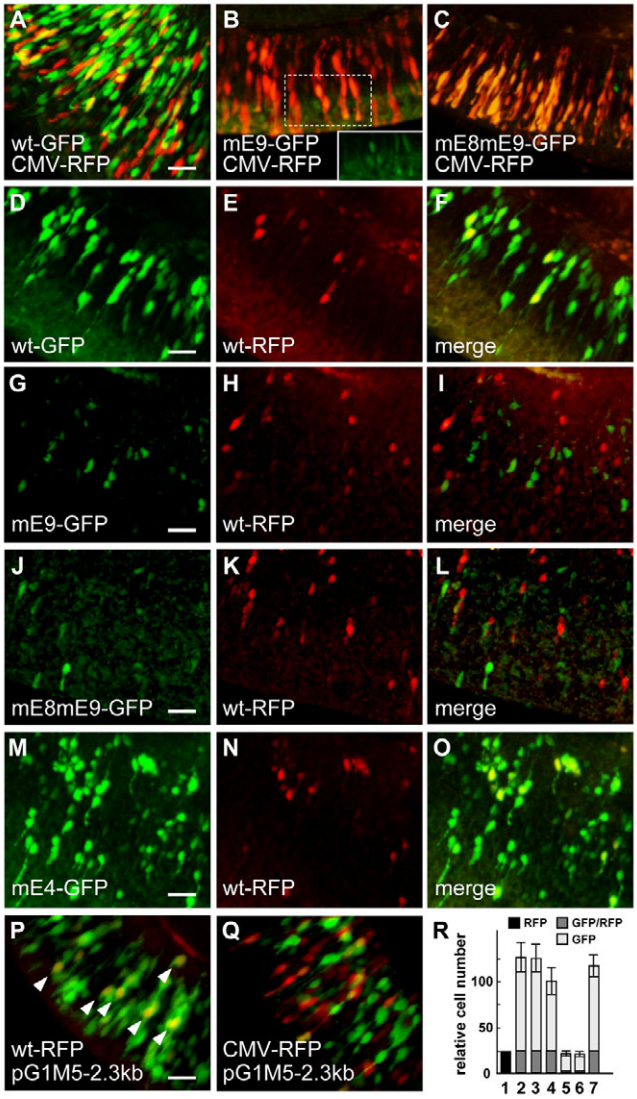

Fig. 5. The E-box E9 mediates the specificity and strength of the chick *Atoh7* promoter in mouse. (**A-Q**) E14.5 mouse retinas were co-electroporated with plasmids as follows: CMV/RFP and $wt_{2.2kb}$/GFP (A) or $mE9_{2.2kb}$/GFP (B) or $mE8mE9_{2.2kb}$/GFP (C) or pG1M5-2.3kb (Q); $wt_{2.2kb}$/RFP and $wt_{2.2kb}$/GFP (D-F) or $mE9_{2.2kb}$/GFP (G-I) or $mE8mE9_{2.2kb}$/GFP (J-L) or $mE4_{2.2kb}$/GFP (M-O) or pG1M5-2.3kb (P). In P, arrowheads indicate cells co-expressing the mouse and chicken promoters. Scale bars: 25 μm. (**R**) Cell numbers obtained with the $wt_{2.2kb}$/RFP plasmid are set at 25 and cell numbers obtained with the wild-type and mutant promoter/GFP plasmids are given relative to this value. 1, $wt_{2.2kb}$/RFP; 2, $wt_{2.2kb}$/GFP; 3, mE4/GFP; 4, mE1mE2/GFP; 5, mE8mE9/GFP; 6, mE9/GFP; 7, pG1M5-2.3kb. Data are presented as the mean ± s.d.; at least three electroporated retinas were analysed per condition.

A

Gene name	ID	retina + Atoh7 vs. retina[1] increase fold change Embryo 1	retina + Atoh7 vs. retina[1] increase fold change Embryo 2	RGC vs. retina[2] increase fold change
Atoh7 (ATH5)	ENSGALG00000003931	62.0178	68.0715	-4.18
Stathmin-2 (SCG10)	ENSGALG00000015736	**2.0478**	**2.5388**	**2.82**
Pleiotrophin (PTN)	ENSGALG00000012893	**1.5266**	**2.9384**	**-2.66**
Cys-Gly rich protein 2	ENSGALG00000010257	1.4810	2.4385	-7.00
Cell cycle protein p38-2G4	ENSGALG00000005980	1.3961	1.9057	-
RNA Binding protein-MS	ENSGALG00000010291	1.2057	2.0146	3.80
SNAP-25 (SNP25)	ENSGALG00000009003	**2.0280**	**1.1235**	**3.30**
ROBO-2	ENSGALG00000015519	**1.2913**	**1.6751**	**2.47**
WDR82	ENSGALG00000003977	1.3355	1.3989	-1.90
KIAA1946	ENSGALG00000002646	1.0725	1.5639	-1.68

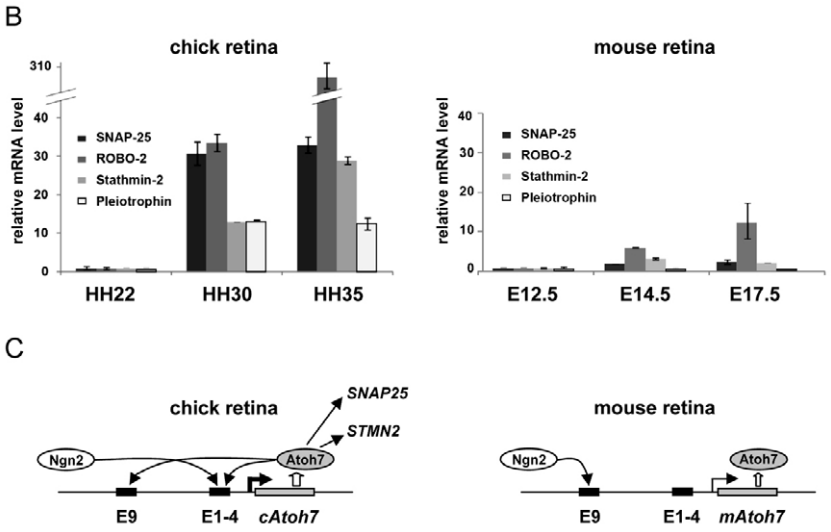

Fig. 6. Identification of genes regulated by Atoh7 in a dose-dependent manner. (**A**) Differentially expressed genes were identified by comparing: (1) a retina overexpressing Atoh7 with the contralateral control retina of two HH22-23 chick embryos; or (2) an enriched population of HH34 RGCs with the total HH34 retina. ArrayExpress accession number E-TABM-417. (**B**) Real-time PCR analysis of transcript levels during embryonic chick and mouse retina development. (**C**) Model illustrating the differential regulation of the chicken and mouse *Atoh7* genes in the developing retina.

3-fold higher in the experimental than in the control retina were processed for Affymetrix gene-chip analysis. This genome-wide screen enabled us to identify genes that were consistently upregulated by chicken Atoh7 (Fig. 6A). Among the best responders, the stathmin 2 (*Stmn2*, *Scg10*) gene was ranked first and is known to regulate microtubule dynamics in neurite growth cones (Greka et al., 2003; Grenningloh et al., 2004; Morii et al., 2006). The much-enriched accumulation of *Stmn2* transcripts in the *lacZ*-expressing cells of HH28 retina transfected with the $wt_{2.2kb}$/lacZ plasmid indicates that *Stmn2* is specifically expressed in Atoh7-expressing cells (see Fig. S8C,D,E in the supplementary material). An Affymetrix gene-chip analysis to compare the transcriptome of immunopanned RGCs with the whole HH34 retina revealed the preferential expression of *Stmn2* in newborn RGCs (Fig. 6A), consistent with the accumulation of *Stmn2* transcripts in the ganglion cell layer (GCL) (see Fig. S9 in the supplementary material) (Hackam et al., 2003). Finally, ChIP assays indicated that the chicken Atoh7 protein was bound to the *Stmn2* promoter in chromatin derived from HH22-23 and HH29-30 retinas (see Fig. S8F in the supplementary material).

Snap25 and *Robo2* transcripts were also enriched in immunopanned RGCs (Fig. 6A) and chicken Atoh7 bound to the *Snap25* promoter region (see Fig. S8F in the supplementary material). At HH29-30, stronger binding of Atoh7 to the *Stmn2* and *Snap25* promoters correlated with the upregulation of Atoh7 (see Fig. S8F in the supplementary material). The expression pattern of pleiotrophin (*Ptn*) showed no evidence for enrichment in Atoh7-expressing cells or in newborn RGCs (Fig. 6A; see Fig. S8E and Fig. S9 in the supplementary material).

To determine whether the expression patterns of the selected candidate genes correlate with the normal kinetics of Atoh7, we compared the expression of *Stmn2*, *Snap25*, *Robo2* and *Ptn* by qPCR during development of the chick and mouse retina (Fig. 6B). In the chick, transcript levels were very low at HH22-23 and the rapid and robust accumulation of transcripts between HH22-23 and HH30 correlated with the upregulation of Atoh7. Moreover, the expression of these genes peaked at stages when the majority of the chicken RGCs extend their axons and develop their dendrites (Fig. 6B) (Rager, 1980). In the mouse, in marked contrast with the dynamic expression profiles seen in the chick, the levels of *Stmn2*, *Snap25*, *Robo2* and *Ptn* transcripts remained steady, or only slightly upregulated, between E12.5 and E17.5, i.e. during the period when mouse RGCs are produced (Fig. 6B). Thus, the expression patterns of these genes are in register with the low expression of mouse Atoh7 (Fig. 1D). These data, together with the fact that the expression of both *Stmn2* and *Snap25* is downregulated in *Math5*$^{-/-}$ mice (Mu et al., 2005), are compatible with the suggestion that these genes might also be targets of Atoh7 in the mouse.

DISCUSSION

Given the crucial role of Atoh7 in the ontogenesis of the vertebrate retina, understanding how its gene is regulated should provide key insights into the transcriptional networks that specify and integrate the RGC lineage within the retina developmental programme. Here, we show how evolutionarily conserved non-coding sequences mediate both the conserved and species-specific transcriptional features of the *Atoh7* gene. The Ngn2 protein maintains the ability to initiate the retina-specific expression of *Atoh7* across distant

species, but diverges in its binding profile to evolutionarily conserved regulatory elements. Our study reveals how such interspecies variations in transcription factor binding cause variations in the activity of the *Atoh7* promoter and how these variations may underlie phenotypic differences between species.

Changes in the binding of Ngn2 and Atoh7 to highly conserved regulatory elements underlie interspecies variations in transcription of the *Atoh7* gene

The onset of Ngn2 and Atoh7 expression in overlapping domains coincide in the chick and mouse retinas, consistent with the co-expression of Ngn2 and Atoh7 in individual chick and mouse progenitor cells (Matter-Sadzinski et al., 2001; Trimarchi et al., 2008). Discrepancies regarding the time of onset of Ngn2 expression between our study and previous reports (Brown et al., 1998; Le et al., 2006) possibly reflect the higher sensitivity of radioactively versus digoxygenin-labelled riboprobes used for the detection of transcripts that accumulate at low levels (Roztocil et al., 1997). The downregulation of Atoh7 expression in $Ngn2^{GFP/GFP}$ mice and its upregulation in chick retina overexpressing Ngn2 (Fig. 1) (Matter-Sadzinski et al., 2005) reveal that the positive regulation of *Atoh7* by Ngn2 is evolutionarily conserved. This regulation correlates with the variable in vivo occupancy by Ngn2 of the *Atoh7* promoter as a function of developmental stage. Although Ngn2 is expressed in many regions of the nervous system anlage, it does not bind the promoter in tissues that do not express Atoh7. In the chick retina, the K4 di- and tri-methylation of histone H3, a modification known to reflect transcriptional competence, increases in exact register with the kinetics of *Atoh7* promoter activity (Skowronska-Krawczyk et al., 2004) (D.S.-K., unpublished data). Likewise, the binding of Ngn2 and its positive effect are associated with chromatin remodelling of the *Atoh7* promoter in the early retina. Surprisingly, despite conservation of the proximal and distal elements, Ngn2 binds the distal sequences in the mouse and the proximal sequences in the chick. In yeast, sequence conservation does not readily predict transcription factor binding sites across related species (Borneman et al., 2007). Our study extends to vertebrates the notion that gene regulation resulting from the pattern of species-specific transcription factor binding to highly conserved regulatory elements may be a cause of divergence between species.

Although the interplay of bHLH proteins at the proximal E-boxes E1, E2 and E4 determines the spatio-temporal specificity of *Atoh7* expression in the chick retina (Hernandez et al., 2007), cooperation between E1, E2, E4 and the conserved distal E-box E9 is required for full-strength promoter activity. Consistent with this notion, mutation of E9 in chick does not alter cell specificity despite a much decreased promoter strength. Our finding that in the mouse retina, E9 sets both the strength of the promoter and its specificity, highlights how the activity of conserved elements depends on the cellular context and may vary between species. In the chick, both Ngn2 and Atoh7 bind the proximal E-boxes and Atoh7 also binds E9. Although we do not exclude the possibility that E9 could mediate competition between Ngn2 and Atoh7, the binding profiles of Atoh7 and Ngn2 proteins suggest that in the early retina, Ngn2 activates transcription of *Atoh7* through the proximal promoter, whereas Atoh7 mediates a positive feedback through E9. This feedback by Atoh7 is moderated by the negative effect that the Hes1 protein exerts upon the proximal promoter, thus keeping the rate of *Atoh7* transcription at a low level in proliferating progenitors (Hernandez et al., 2007). The downregulation of Hes1 in Atoh7-expressing cells that exit the cell cycle coincides with the rapid upregulation of Atoh7. This upregulation is mediated by Atoh7 and Ngn2, which drive the promoter at peak activity through the combinatorial use of E2, E4 and E9 (Fig. 6C). In $Hes1^{-/-}$ mice, precocious peripheral expansion of the Atoh7 expression domain takes place in the retina (Lee et al., 2005).

Consistent with the dominant effect of E9, Ngn2 exclusively binds the distal region in mouse (Fig. 2B). The striking difference in the functional properties of E9 between mouse and chicken does not result from sequence variations; it might reflect epigenetic differences, as chromatin modifications correlate with the binding of bHLH proteins (Skowronska-Krawczyk et al., 2004). The fact that Ngn2 expression is low in the mouse retina, whereas it is strongly upregulated in the chick retina (Fig. 1D,E) (Matter-Sadzinski et al., 2001), suggests the interesting possibility that the proximal and distal promoter regions are selected by Ngn2 in a dose-dependent manner. Recruitment of the protein on both the distal and proximal promoter regions in mouse P19 cells that overexpress Ngn2 (Fig. 2C) is consistent with this notion. The distal and proximal E-boxes have different sequence identities and their affinity for Ngn2 may thus be sequence dependent, as shown for Atoh7 (Hernandez et al., 2007). Wilson et al. have shown that instructions to direct transcription of human chromosome 21 in mouse hepatocytes are primarily context independent and are thus mediated by the DNA sequence (Wilson et al., 2008). Our finding that the chick *Atoh7* promoter in the mouse, or the mouse *Atoh7* promoter in the chick, displays the activity features of the host suggests, however, that the cellular context can influence transcription in the developing nervous system.

Consistent with the role of E9 ascertained in this report, a 0.6 kb sequence encompassing the proximal E-boxes has no promoter activity in transgenic mice, whereas a 2.3 kb sequence that includes E8 and E9 (see Fig. S2C in the supplementary material) is sufficient to recapitulate in full the endogenous Atoh7 expression in the E11.5 mouse retina (Hufnagel et al., 2007; Hutcheson et al., 2005).

The maintenance of Atoh7 expression in $Math5^{-/-}$ mice (Brown et al., 2001; Wang et al., 2001) rules out a positive feedback in this species. Thus, the interplay of Ngn2 and Atoh7 at the proximal promoter seen in the chick (Fig. 6C) (Hernandez et al., 2007) might not occur in the mouse retina. Instead, the Ngn2 protein, acting through the distal promoter, mediates the low expression of Atoh7 seen in mouse during the period of development when RGCs are produced. The residual, but significant, expression of *Atoh7* in $Ngn2^{GFP/GFP}$ mice suggests that other transcription factors might intervene in the regulation of this gene. Pax6 is necessary for Atoh7 expression in the mouse (Brown et al., 1998; Marquardt et al., 2001; Riesenberg et al., 2009), but cannot by itself control the spatio-temporal and cell cycle phase expression of Atoh7 (Riesenberg et al., 2009). In *Xenopus*, Pax6 binding sites within a distal enhancer are required for its enhancer activity (Willardsen et al., 2009). However, Pax6 alone is not sufficient to induce ectopic expression of *Xenopus* Atoh7. The fact that the distal enhancer in *Xenopus* does not require E8 and E9 [respectively E3 and E4 in Willardsen et al. (Willardsen et al., 2009)] extends to lower vertebrates the notion that conserved E-boxes assume different roles in different species.

There is no obvious abnormality of the GCL in $Ngn2^{GFP/GFP}$ mice (D.S.-K., unpublished), despite the downregulation of Atoh7. However, we cannot exclude the possibility that the GCL might be populated with other cell types, such as amacrine cells, or that different ratios of the numerous RGC subclasses might be produced in response to different levels of Atoh7.

Atoh7 regulates a set of genes that underlie phenotypic divergence between mouse and chick

Our study reveals that highly conserved non-coding sequences mediate non-conserved interplays of bHLH proteins at the *Atoh7* promoter. The proximal E-boxes E1, E2 and E4 mediate activation by Ngn2 and, in addition, the positive feedback by Atoh7 acting upon E9 reinforces Atoh7 expression during the first phase of chick retina development. Expression of Atoh7 is at least 10-fold higher in chick than in mouse early retina (Fig. 1D,E), where mouse Ngn2 effects a weak activation through the distal promoter. RGCs are massively produced in the chick retina [~2.5×10^6 RGCs/chicken retina (Rager, 1980) versus ~7×10^4 RGCs/mouse retina (Erkman et al., 2000)] and the ratio of RGCs to photoreceptors is ~25-fold higher in the avian than in the mouse retina (Rahman et al., 2007; Jeon et al., 1998). We suggest that the much-enhanced expression of Atoh7 in the chick promotes the recruitment to the RGC lineage of a larger set of retinal progenitors.

Later, at the time when the majority of RGCs exit the cell cycle and differentiate, the interaction of the Atoh7 protein at E2, E4 and E9 mediates a strong positive feedback (Fig. 6C). This occurs in the chick but not in the mouse retina, raising the question of why such a transient Atoh7 upregulation is needed to produce RGCs in the chick. Part of the answer might reside in the coherent set of genes that are expressed in newborn RGCs and are regulated by Atoh7 in a dose-dependent manner. Proteins encoded by *Stmn2*, *Snap25*, *Robo2* and *Ptn* are protagonists in signalling pathways that link external stimuli to processes such as growth cone protrusion, axonal pathfinding and initial formation of synaptic contacts. The stathmin proteins regulate microtubule dynamics and Stmn2 is highly expressed during neuronal development and is enriched in growth cones (Greka et al., 2003; Grenningloh et al., 2004; Morii et al., 2006). The Snap25 proteins are components of the synaptic vesicle exocytotic machinery and participate in neurite outgrowth (Delgado-Martinez et al., 2007; Waites et al., 2005). Robo2 plays a role in the axonal pathfinding of RGCs (Campbell et al., 2007). The regulation of the corresponding genes by Atoh7 suggests that the protein might directly control the development of dendritic arbors and axons in newborn RGCs.

Ramon y Cajal (Bergua, 1994) noted early on that the avian retina is the most complicated with respect to the morphology of the RGCs. Screens of the dendritic patterns of RGCs have revealed that whereas the large majority of RGCs are monostratified in the mouse retina (Kong et al., 2005), bi- and tristratification patterns predominate in the chicken retina (Naito and Chen, 2004). A recent report brought into focus a novel mechanism whereby dendritic stratification of RGCs is achieved (Mumm et al., 2006). In that study, in vivo time-lapse imaging was used to show that zebrafish RGCs display early patterns of dendritic outgrowth that are predictive of their final lamination, rather than lamination resulting from the pruning of initially exuberant arbors, as generally accepted. We propose that mouse RGCs might develop simpler dendritic patterns as a result of the low expression of neurite outgrowth-associated proteins.

Acknowledgements

We thank D. Duboule and C. Pournaras for space, support and encouragement; M. Krawczyk for advice on EMSA and critical reading of the manuscript; M. Vetter for plasmid pG1M5-2.3kb; P. Descombes, O. Schaad, M. Docquier and D. Chollet (Genomics Platform, NCCR Frontiers in Genetics, University of Geneva) for assistance that was essential for our microarray analysis; and F. Ilias, I. Weissbrodt and N. Taverney for technical help. Confocal microscopy was performed at the Bioimaging Platform, NCCR Frontiers in Genetics, with the kind help of C. Bauer. The Swiss National Science Foundation, the Ohayon Foundation, the Provisu Foundation and the State of Geneva support our laboratory.

Supplementary material

Supplementary material for this article is available at http://dev.biologists.org/cgi/content/full/136/22/3767/DC1

References

Altschul, S. F., Madden, T. L., Schaffer, A. A., Zhang, J., Zhang, Z., Miller, W. and Lipman, D. J. (1997). Gapped BLAST and PSI-BLAST: a new generation of protein database search programs. *Nucleic Acids Res.* **25**, 3389-3402.

Bergua, A. (1994). The retina of the vertebrates by Santiago Ramon y Cajal – 100 years in German translation. *Klin. Monatsbl. Augenheilkd.* **205**, 372-373.

Birney, E., Stamatoyannopoulos, J. A., Dutta, A., Guigo, R., Gingeras, T. R., Margulies, E. H., Weng, Z., Snyder, M., Dermitzakis, E. T., Thurman, R. E. et al. (2007). Identification and analysis of functional elements in 1% of the human genome by the ENCODE pilot project. *Nature* **447**, 799-816.

Borneman, A. R., Gianoulis, T. A., Zhang, Z. D., Yu, H., Rozowsky, J., Seringhaus, M. R., Wang, L. Y., Gerstein, M. and Snyder, M. (2007). Divergence of transcription factor binding sites across related yeast species. *Science* **317**, 815-819.

Brown, N. L., Kanekar, S., Vetter, M. L., Tucker, P. K., Gemza, D. L. and Glaser, T. (1998). Math5 encodes a murine basic helix-loop-helix transcription factor expressed during early stages of retinal neurogenesis. *Development* **125**, 4821-4833.

Brown, N. L., Patel, S., Brzezinski, J. and Glaser, T. (2001). Math5 is required for retinal ganglion cell and optic nerve formation. *Development* **128**, 2497-2508.

Brown, N. L., Dagenais, S. L., Chen, C. M. and Glaser, T. (2002). Molecular characterization and mapping of ATOH7, a human atonal homolog with a predicted role in retinal ganglion cell development. *Mamm. Genome* **13**, 95-101.

Brudno, M., Do, C. B., Cooper, G. M., Kim, M. F., Davydov, E., Green, E. D., Sidow, A. and Batzoglou, S. (2003). LAGAN and Multi-LAGAN: efficient tools for large-scale multiple alignment of genomic DNA. *Genome Res.* **13**, 721-731.

Brzezinski, J. A., IV, Brown, N. L., Tanikawa, A., Bush, R. A., Sieving, P. A., Vitaterna, M. H., Takahashi, J. S. and Glaser, T. (2005). Loss of circadian photoentrainment and abnormal retinal electrophysiology in Math5 mutant mice. *Invest. Ophthalmol. Vis. Sci.* **46**, 2540-2551.

Campbell, D. S., Stringham, S. A., Timm, A., Xiao, T., Law, M. Y., Baier, H., Nonet, M. L. and Chien, C. B. (2007). Slit1a inhibits retinal ganglion cell arborization and synaptogenesis via Robo2-dependent and -independent pathways. *Neuron* **55**, 231-245.

Castro, D. S., Skowronska-Krawczyk, D., Armant, O., Donaldson, I. J., Parras, C., Hunt, C., Critchley, J. A., Nguyen, L., Gossler, A., Gottgens, B. et al. (2006). Proneural bHLH and Brn proteins coregulate a neurogenic program through cooperative binding to a conserved DNA motif. *Dev. Cell* **11**, 831-844.

Davidson, E. H., Rast, J. P., Oliveri, P., Ransick, A., Calestani, C., Yuh, C. H., Minokawa, T., Amore, G., Hinman, V., Arenas-Mena, C. et al. (2002). A genomic regulatory network for development. *Science* **295**, 1669-1678.

Delgado-Martinez, I., Nehring, R. B. and Sorensen, J. B. (2007). Differential abilities of SNAP-25 homologs to support neuronal function. *J. Neurosci.* **27**, 9380-9391.

Erkman, L., Yates, P. A., McLaughlin, T., McEvilly, R. J., Whisenhunt, T., O'Connell, S. M., Krones, A. I., Kirby, M. A., Rapaport, D. H., Bermingham, J. R. et al. (2000). A POU domain transcription factor-dependent program regulates axon pathfinding in the vertebrate visual system. *Neuron* **28**, 779-792.

Farah, M. H., Olson, J. M., Sucic, H. B., Hume, R. I., Tapscott, S. J. and Turner, D. L. (2000). Generation of neurons by transient expression of neural bHLH proteins in mammalian cells. *Development* **127**, 693-702.

Fode, C., Ma, Q., Casarosa, S., Ang, S. L., Anderson, D. J. and Guillemot, F. (2000). A role for neural determination genes in specifying the dorsoventral identity of telencephalic neurons. *Genes Dev.* **14**, 67-80.

Greka, A., Navarro, B., Oancea, E., Duggan, A. and Clapham, D. E. (2003). TRPC5 is a regulator of hippocampal neurite length and growth cone morphology. *Nat. Neurosci.* **6**, 837-845.

Grenningloh, G., Soehrman, S., Bondallaz, P., Ruchti, E. and Cadas, H. (2004). Role of the microtubule destabilizing proteins SCG10 and stathmin in neuronal growth. *J. Neurobiol.* **58**, 60-69.

Hackam, A. S., Bradford, R. L., Bakhru, R. N., Shah, R. M., Farkas, R., Zack, D. J. and Adler, R. (2003). Gene discovery in the embryonic chick retina. *Mol. Vis.* **9**, 262-276.

Hamburger, V. and Hamilton, H. L. (1951). A series of normal stages in the development of the chick embryo. *J. Morphol.* **88**, 49-92.

Heng, J. I., Nguyen, L., Castro, D. S., Zimmer, C., Wildner, H., Armant, O., Skowronska-Krawczyk, D., Bedogni, F., Matter, J. M., Hevner, R. et al. (2008). Neurogenin 2 controls cortical neuron migration through regulation of Rnd2. *Nature* **455**, 114-118.

Hernandez, J., Matter-Sadzinski, L., Skowronska-Krawczyk, D., Chiodini, F., Alliod, C., Ballivet, M. and Matter, J. M. (2007). Highly conserved sequences mediate the dynamic interplay of basic helix-loop-helix proteins regulating retinogenesis. *J. Biol. Chem.* **282**, 37894-37905.

Hufnagel, R. B., Riesenberg, A. N., Saul, S. M. and Brown, N. L. (2007). Conserved regulation of Math5 and Math1 revealed by Math5-GFP transgenes. *Mol. Cell. Neurosci.* **36**, 435-448.
Hutcheson, D. A., Hanson, M. I., Moore, K. B., Le, T. T., Brown, N. L. and Vetter, M. L. (2005). bHLH-dependent and -independent modes of Ath5 gene regulation during retinal development. *Development* **132**, 829-839.
Jeon, C. J., Strettoi, E. and Masland, R. H. (1998). The major cell populations of the mouse retina. *J. Neurosci.* **18**, 8936-8946.
Kanekar, S., Perron, M., Dorsky, R., Harris, W. A., Jan, L. Y., Jan, Y. N. and Vetter, M. L. (1997). Xath5 participates in a network of bHLH genes in the developing Xenopus retina. *Neuron* **19**, 981-994.
Kay, J. N., Finger-Baier, K. C., Roeser, T., Staub, W. and Baier, H. (2001). Retinal ganglion cell genesis requires lakritz, a zebrafish atonal homolog. *Neuron* **30**, 725-736.
Kong, J. H., Fish, D. R., Rockhill, R. L. and Masland, R. H. (2005). Diversity of ganglion cells in the mouse retina: Unsupervised morphological classification and its limits. *J. Comp. Neurol.* **489**, 293-310.
Le, T. T., Wroblewski, E., Patel, S., Riesenberg, A. N. and Brown, N. L. (2006). Math5 is required for both early retinal neuron differentiation and cell cycle progression. *Dev. Biol.* **295**, 764-778.
Lee, H. Y., Wroblewski, E., Philips, G. T., Stair, C. N., Conley, K., Reedy, M., Mastick, G. S. and Brown, N. L. (2005). Multiple requirements for Hes 1 during early eye formation. *Dev. Biol.* **284**, 464-478.
Liu, W., Mo, Z. and Xiang, M. (2001). The Ath5 proneural genes function upstream of Brn3 POU domain transcription factor genes to promote retinal ganglion cell development. *Proc. Natl. Acad. Sci. USA* **98**, 1649-1654.
Livesey, F. J. and Cepko, C. L. (2001). Vertebrate neural cell-fate determination: lessons from the retina. *Nat. Rev. Neurosci.* **2**, 109-118.
Lo, L., Dormand, E., Greenwood, A. and Anderson, D. J. (2002). Comparison of the generic neuronal differentiation and neuron subtype specification functions of mammalian achaete-scute and atonal homologs in cultured neural progenitor cells. *Development* **129**, 1553-1567.
Marquardt, T., Ashery-Padan, R., Andrejewski, N., Scardigli, R., Guillemot, F. and Gruss, P. (2001). Pax6 is required for the multipotent state of retinal progenitor cells. *Cell* **105**, 43-55.
Masland, R. H. (2001). The fundamental plan of the retina. *Nat. Neurosci.* **4**, 877-886.
Matter-Sadzinski, L., Matter, J. M., Ong, M. T., Hernandez, J. and Ballivet, M. (2001). Specification of neurotransmitter receptor identity in developing retina: the chick ATH5 promoter integrates the positive and negative effects of several bHLH proteins. *Development* **128**, 217-231.
Matter-Sadzinski, L., Puzianowska-Kuznicka, M., Hernandez, J., Ballivet, M. and Matter, J. M. (2005). A bHLH transcriptional network regulating the specification of retinal ganglion cells. *Development* **132**, 3907-3921.
Matys, V., Fricke, E., Geffers, R., Gossling, E., Haubrock, M., Hehl, R., Hornischer, K., Karas, D., Kel, A. E., Kel-Margoulis, O. V. et al. (2003). TRANSFAC: transcriptional regulation, from patterns to profiles. *Nucleic Acids Res.* **31**, 374-378.
Morii, H., Shiraishi-Yamaguchi, Y. and Mori, N. (2006). SCG10, a microtubule destabilizing factor, stimulates the neurite outgrowth by modulating microtubule dynamics in rat hippocampal primary cultured neurons. *J. Neurobiol.* **66**, 1101-1114.
Mu, X., Fu, X., Sun, H., Beremand, P. D., Thomas, T. L. and Klein, W. H. (2005). A gene network downstream of transcription factor Math5 regulates retinal progenitor cell competence and ganglion cell fate. *Dev. Biol.* **280**, 467-481.
Mumm, J. S., Williams, P. R., Godinho, L., Koerber, A., Pittman, A. J., Roeser, T., Chien, C. B., Baier, H. and Wong, R. O. (2006). In vivo imaging reveals dendritic targeting of laminated afferents by zebrafish retinal ganglion cells. *Neuron* **52**, 609-621.
Naito, J. and Chen, Y. (2004). Morphologic analysis and classification of ganglion cells of the chick retina by intracellular injection of Lucifer Yellow and retrograde labeling with DiI. *J. Comp. Neurol.* **469**, 360-376.
Rager, G. H. (1980). Development of the retinotectal projection in the chicken. *Adv. Anat. Embryol. Cell Biol.* **63**, I-VIII, 1-90.
Rahman, M. L., Aoyama, M. and Sugita, S. (2007). Number and density of retinal photoreceptor cells with emphasis on oil droplet distribution in the Mallard Duck (*Anas platyrhynchos* var. *domesticus*). *Animal Sci. J.* **78**, 639-649.
Rahmann, S., Muller, T. and Vingron, M. (2003). On the power of profiles for transcription factor binding site detection. *Stat. Appl. Genet. Mol. Biol.* **2**, Article7.
Riesenberg, A. N., Le, T. T., Willardsen, M. I., Blackburn, D. C., Vetter, M. L. and Brown, N. L. (2009). Pax6 regulation of Math5 during mouse retinal neurogenesis. *Genesis* **47**, 175-187.
Roztocil, T., Matter-Sadzinski, L., Alliod, C., Ballivet, M. and Matter, J. M. (1997). NeuroM, a neural helix-loop-helix transcription factor, defines a new transition stage in neurogenesis. *Development* **124**, 3263-3272.
Sandmann, T., Girardot, C., Brehme, M., Tongprasit, W., Stolc, V. and Furlong, E. E. (2007). A core transcriptional network for early mesoderm development in Drosophila melanogaster. *Genes Dev.* **21**, 436-449.
Schmidt, E. E. and Schibler, U. (1995). Cell size regulation, a mechanism that controls cellular RNA accumulation: consequences on regulation of the ubiquitous transcription factors Oct1 and NF-Y and the liver-enriched transcription factor DBP. *J. Cell Biol.* **128**, 467-483.
Schroeder, M. D., Pearce, M., Fak, J., Fan, H., Unnerstall, U., Emberly, E., Rajewsky, N., Siggia, E. D. and Gaul, U. (2004). Transcriptional control in the segmentation gene network of Drosophila. *PLoS Biol.* **2**, E271.
Seibt, J., Schuurmans, C., Gradwhol, G., Dehay, C., Vanderhaeghen, P., Guillemot, F. and Polleux, F. (2003). Neurogenin2 specifies the connectivity of thalamic neurons by controlling axon responsiveness to intermediate target cues. *Neuron* **39**, 439-452.
Skowronska-Krawczyk, D., Ballivet, M., Dynlacht, B. D. and Matter, J. M. (2004). Highly specific interactions between bHLH transcription factors and chromatin during retina development. *Development* **131**, 4447-4454.
Skowronska-Krawczyk, D., Matter-Sadzinski, L., Ballivet, M. and Matter, J. M. (2005). The basic domain of ATH5 mediates neuron-specific promoter activity during retina development. *Mol. Cell. Biol.* **25**, 10029-10039.
Sonnhammer, E. L. and Durbin, R. (1995). A dot-matrix program with dynamic threshold control suited for genomic DNA and protein sequence analysis. *Gene.* **167**, GC1-GC10.
Sun, Y., Kanekar, S. L., Vetter, M. L., Gorski, S., Jan, Y. N., Glaser, T. and Brown, N. L. (2003). Conserved and divergent functions of Drosophila atonal, amphibian, and mammalian Ath5 genes. *Evol. Dev.* **5**, 532-541.
Trimarchi, J. M., Stadler, M. B. and Cepko, C. L. (2008). Individual retinal progenitor cells display extensive heterogeneity of gene expression. *PLoS ONE* **3**, e1588.
Waites, C. L., Craig, A. M. and Garner, C. C. (2005). Mechanisms of vertebrate synaptogenesis. *Annu. Rev. Neurosci.* **28**, 251-274.
Wang, S. W., Kim, B. S., Ding, K., Wang, H., Sun, D., Johnson, R. L., Klein, W. H. and Gan, L. (2001). Requirement for math5 in the development of retinal ganglion cells. *Genes Dev.* **15**, 24-29.
Willardsen, M. I., Suli, A., Pan, Y., Marsh-Armstrong, N., Chien, C. B., El-Hodiri, H., Brown, N. L., Moore, K. B. and Vetter, M. L. (2009). Temporal regulation of Ath5 gene expression during eye development. *Dev. Biol.* **326**, 471-481.
Wilson, M. D., Barbosa-Morais, N. L., Schmidt, D., Conboy, C. M., Vanes, L., Tybulewicz, V. L., Fisher, E. M., Tavare, S. and Odom, D. T. (2008). Species-specific transcription in mice carrying human chromosome 21. *Science* **322**, 434-438.
Wuarin, J. and Schibler, U. (1994). Physical isolation of nascent RNA chains transcribed by RNA polymerase II: evidence for cotranscriptional splicing. *Mol. Cell. Biol.* **14**, 7219-7225.
Yang, Z., Ding, K., Pan, L., Deng, M. and Gan, L. (2003). Math5 determines the competence state of retinal ganglion cell progenitors. *Dev. Biol.* **264**, 240-254.

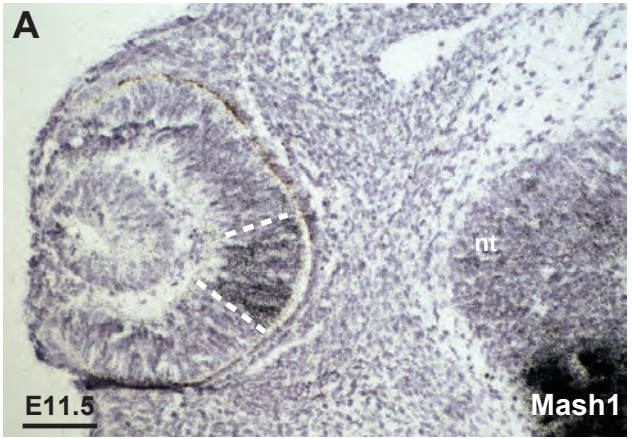
A
nt
E11.5
Mash1

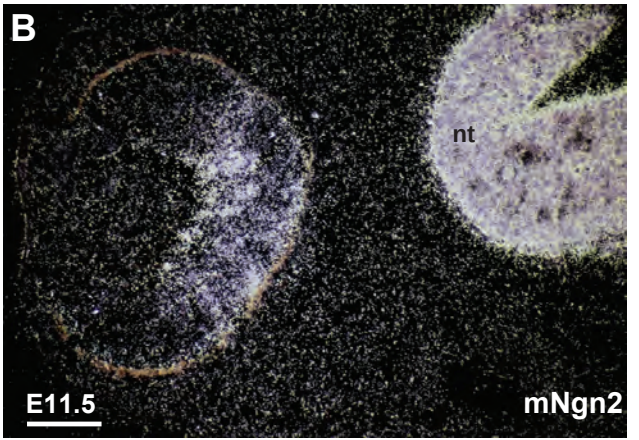
B
nt
E11.5
mNgn2

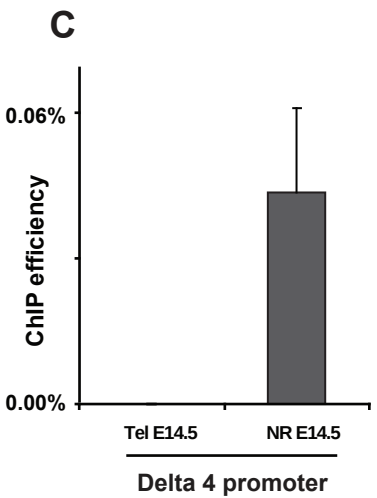
C
0.06%
0.00%
ChIP efficiency
Tel E14.5
NR E14.5
Delta 4 promoter

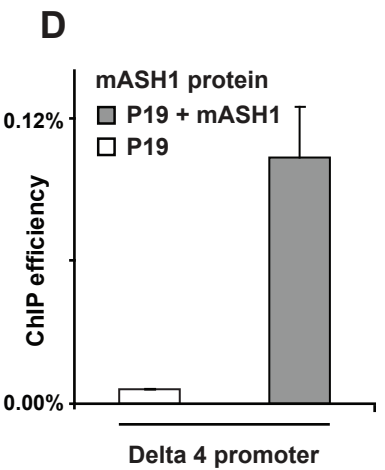
D
mASH1 protein
P19 + mASH1
P19
0.12%
0.00%
ChIP efficiency
Delta 4 promoter

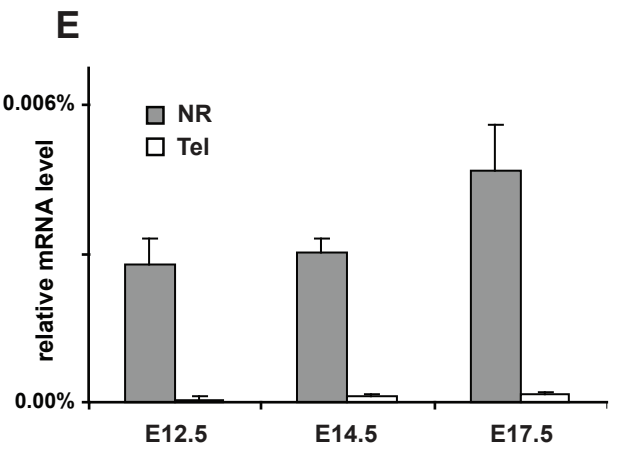
E
0.006%
0.00%
relative mRNA level
NR
Tel
E12.5
E14.5
E17.5

Figure S2

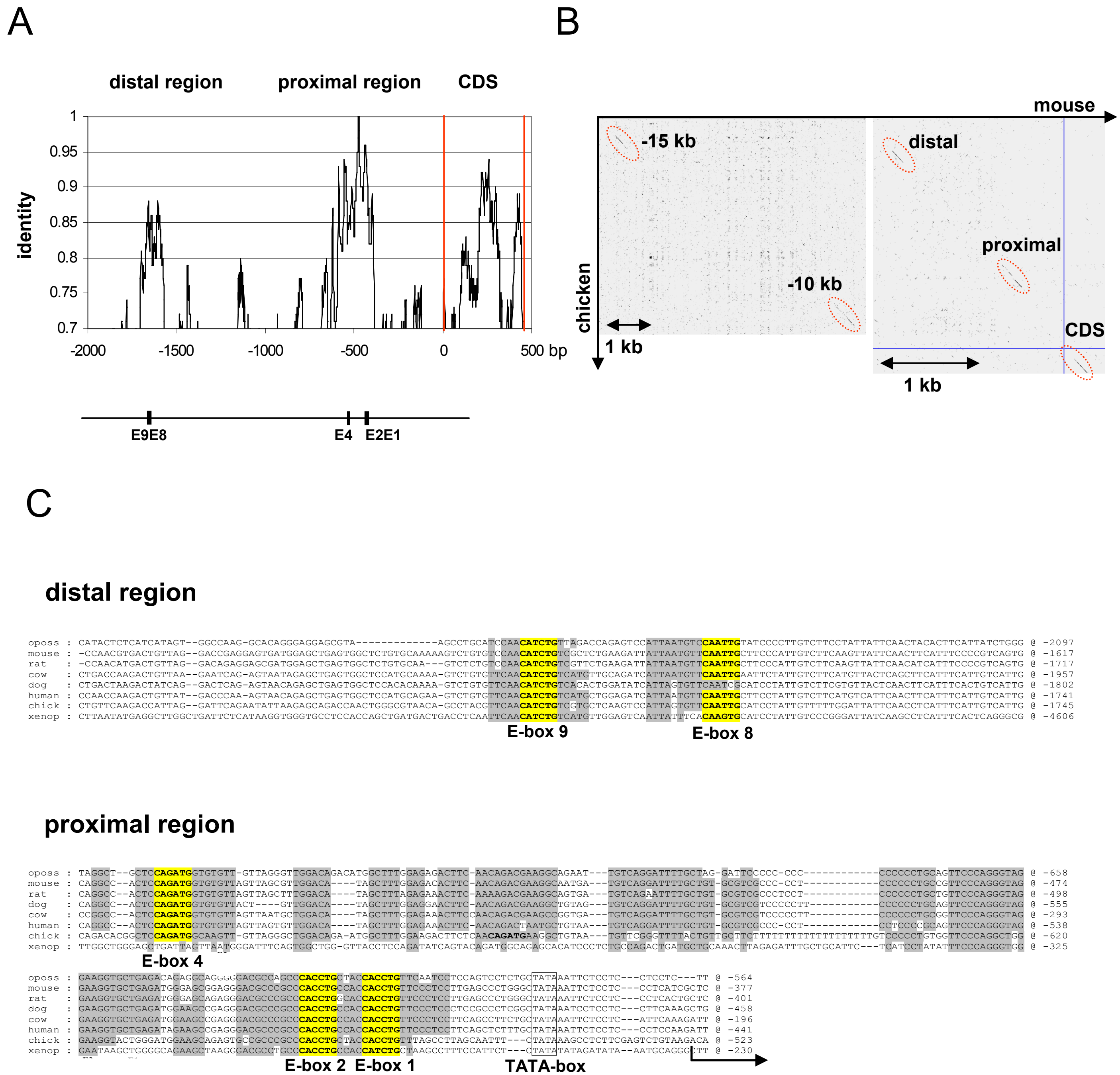

A
distal region
proximal region
CDS
identity
1
0.95
0.9
0.85
0.8
0.75
0.7
-2000
-1500
-1000
-500
0
500 bp
E9E8
E4
E2E1
B
mouse
chicken
-15 kb
-10 kb
1 kb
distal
proximal
CDS
1 kb
C
distal region
oposs
mouse
rat
cow
dog
human
chick
xenop
E-box 9
E-box 8
proximal region
E-box 4
E-box 2
E-box 1
TATA-box

FIGURE S3

^{32}P-probe	wild-type						
hAtoh7			+	+	+	+	+
GFP		+					
Ab				M01	M02	poly	IgG

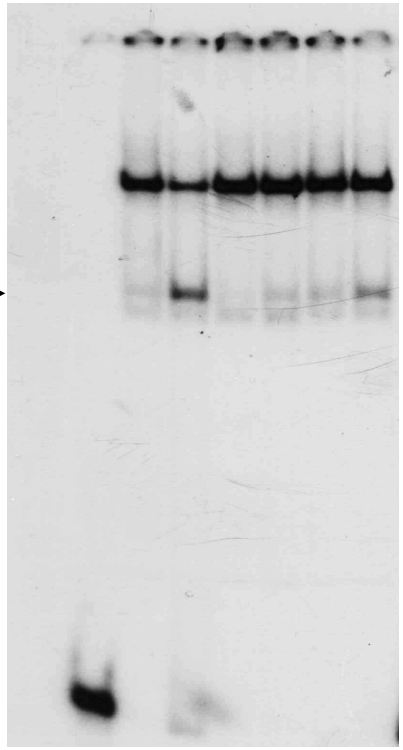

Free probe

Figure S4

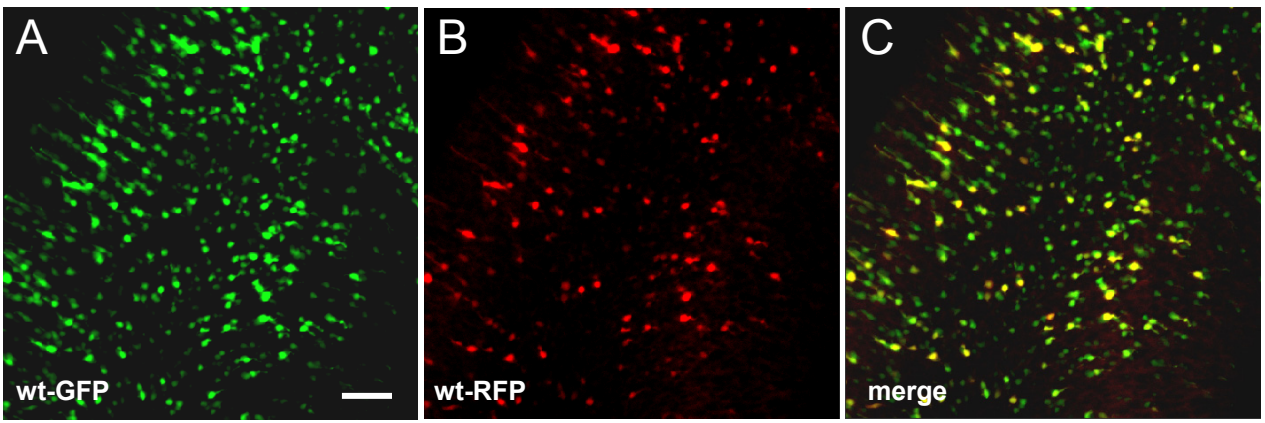
A
wt-GFP
B
wt-RFP
C
merge

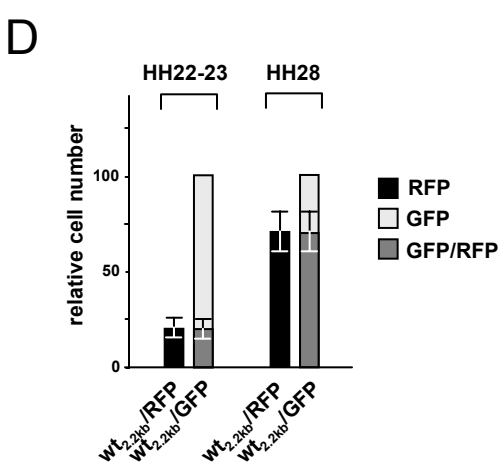
D
HH22-23
HH28
relative cell number
100
50
0
RFP
GFP
GFP/RFP
wt2.2kb/RFP
wt2.2kb/GFP
wt2.2kb/RFP
wt2.2kb/GFP

Figure S5

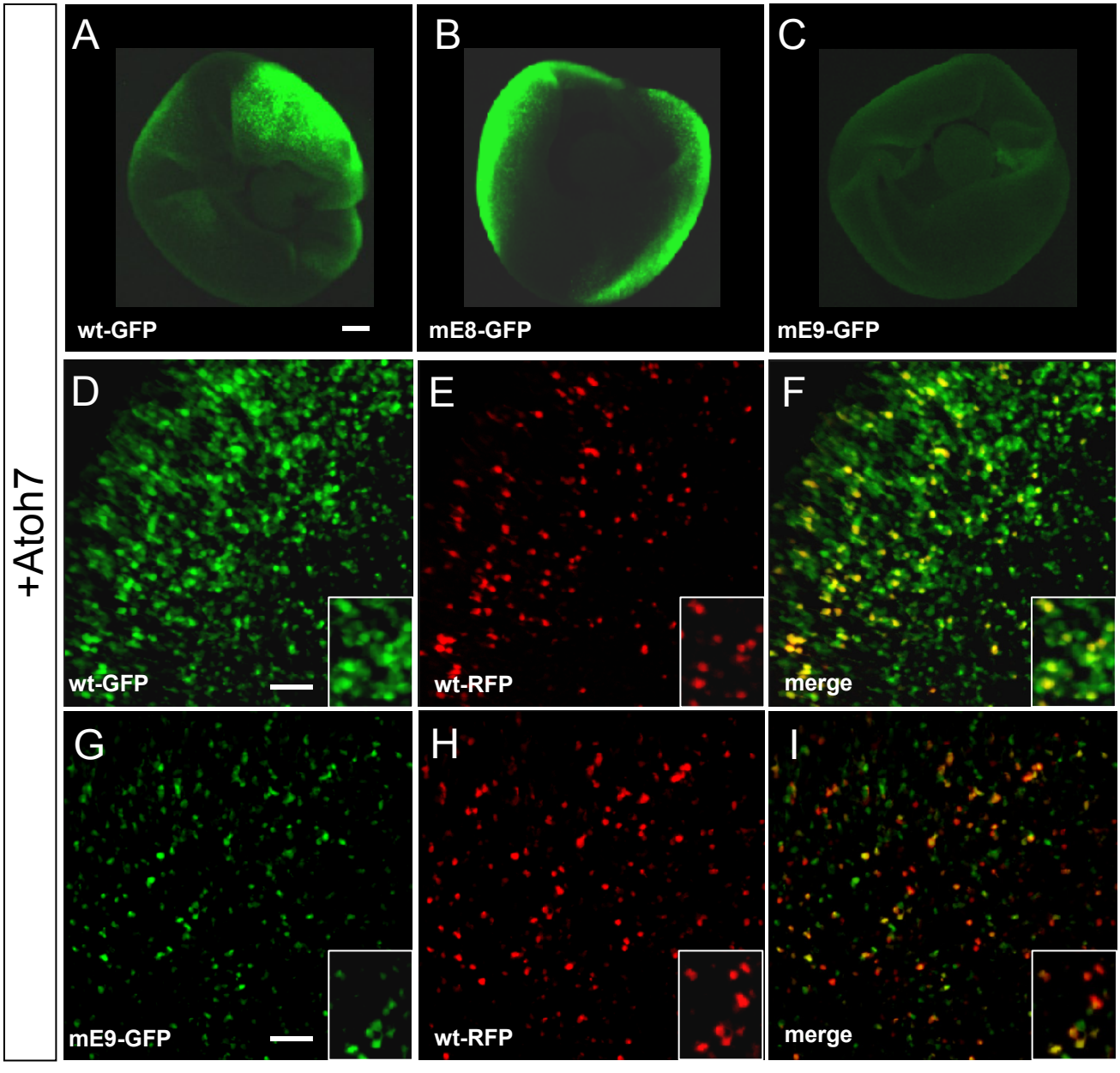
+Atoh7
A
wt-GFP
B
mE8-GFP
C
mE9-GFP
D
wt-GFP
E
wt-RFP
F
merge
G
mE9-GFP
H
wt-RFP
I
merge

J

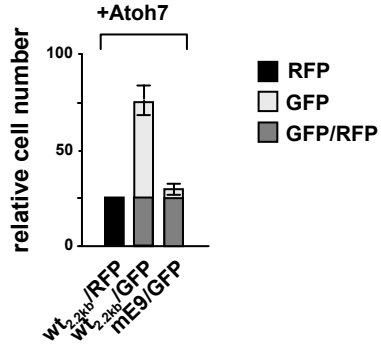
+Atoh7
relative cell number
100
50
0
RFP
GFP
GFP/RFP
wt2.2kb/RFP
wt2.2kb/GFP
mE9/GFP

Figure S6

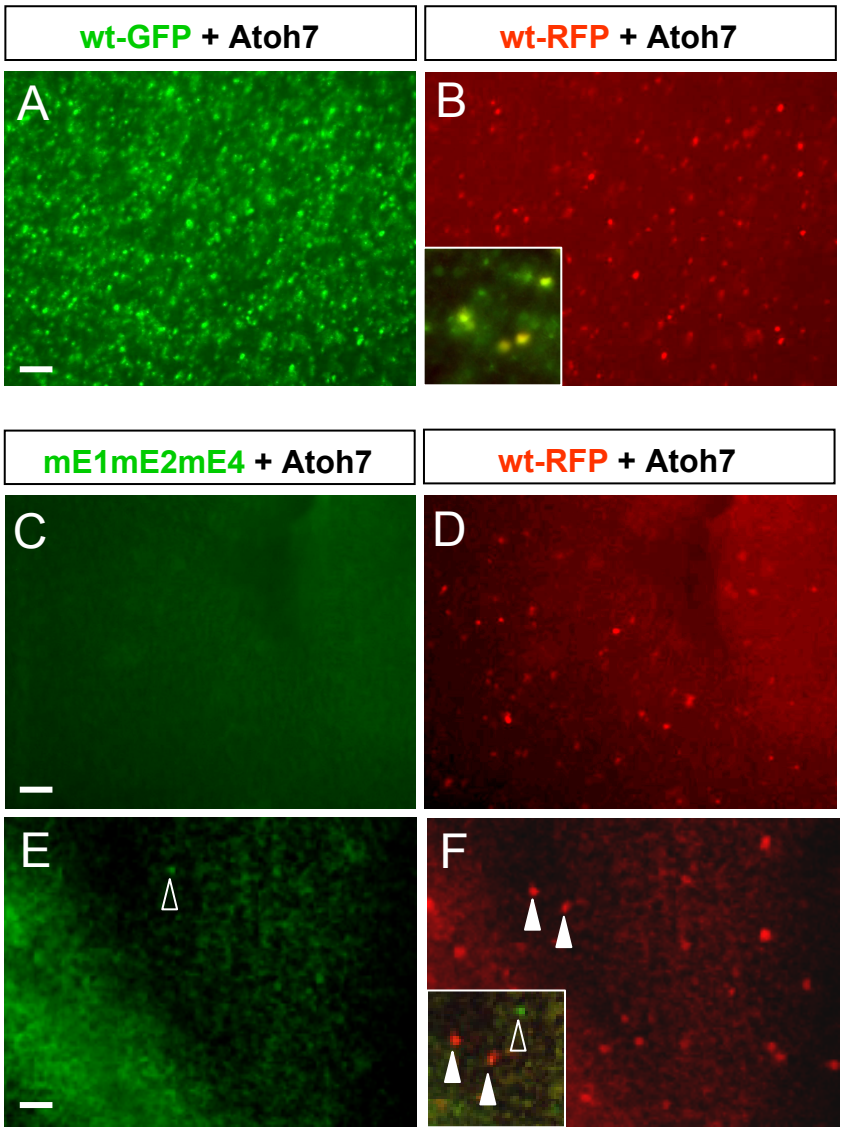
wt-GFP + Atoh7
wt-RFP + Atoh7
A
B
mE1mE2mE4 + Atoh7
wt-RFP + Atoh7
C
D
E
F

Figure S7

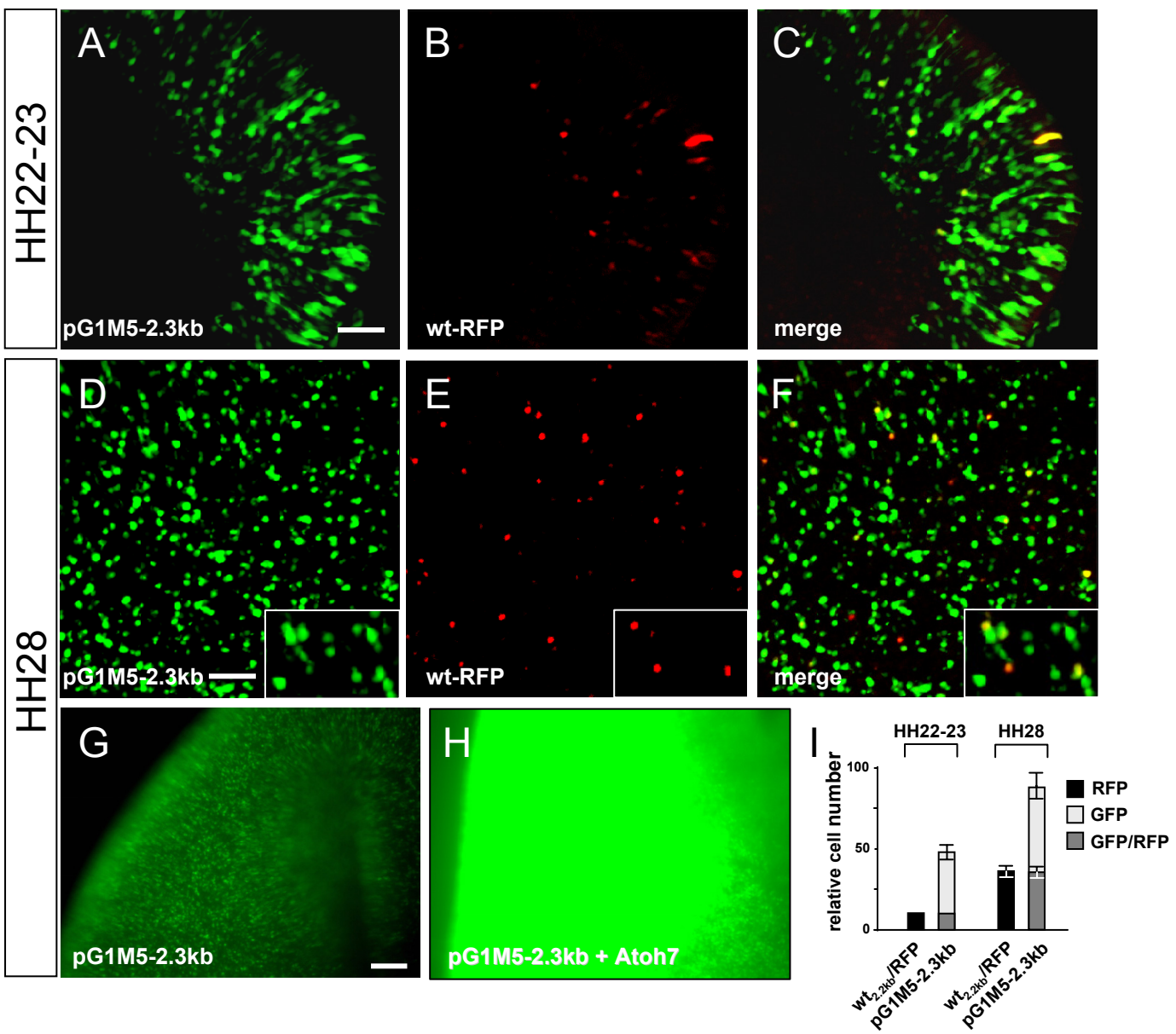
HH22-23
A
pG1M5-2.3kb
B
wt-RFP
C
merge
HH28
D
pG1M5-2.3kb
E
wt-RFP
F
merge
G
pG1M5-2.3kb
H
pG1M5-2.3kb + Atoh7
I
HH22-23
HH28
relative cell number
100
50
0
RFP
GFP
GFP/RFP
wt2.2kb/RFP
pG1M5-2.3kb
wt2.2kb/RFP
pG1M5-2.3kb

Figure S8

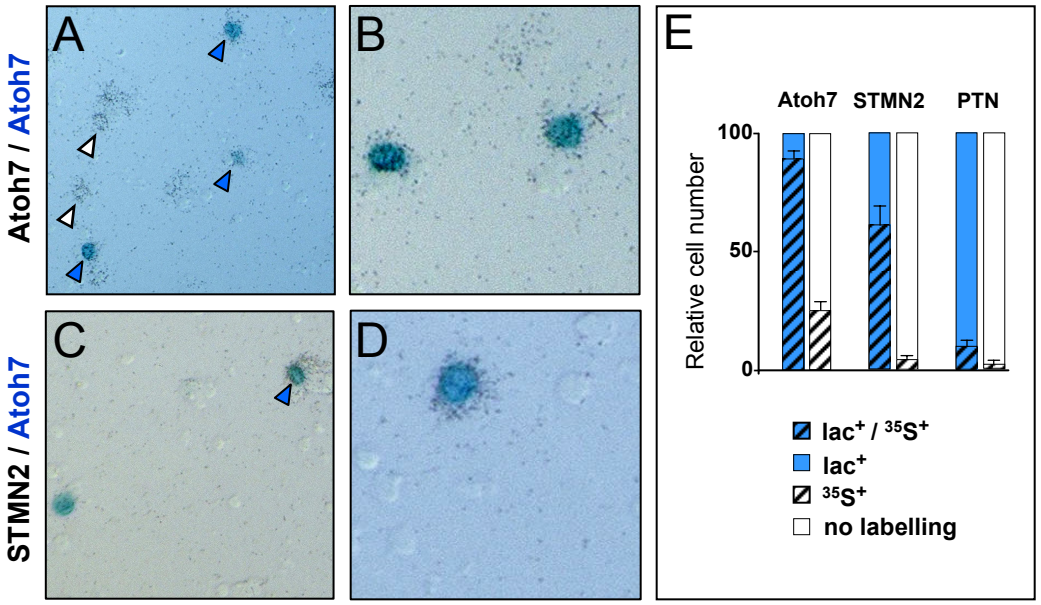
A
B
C
D
Atoh7 / Atoh7
STMN2 / Atoh7
E
Atoh7
STMN2
PTN
100
50
0
Relative cell number
lac+ / 35S+
lac+
35S+
no labelling

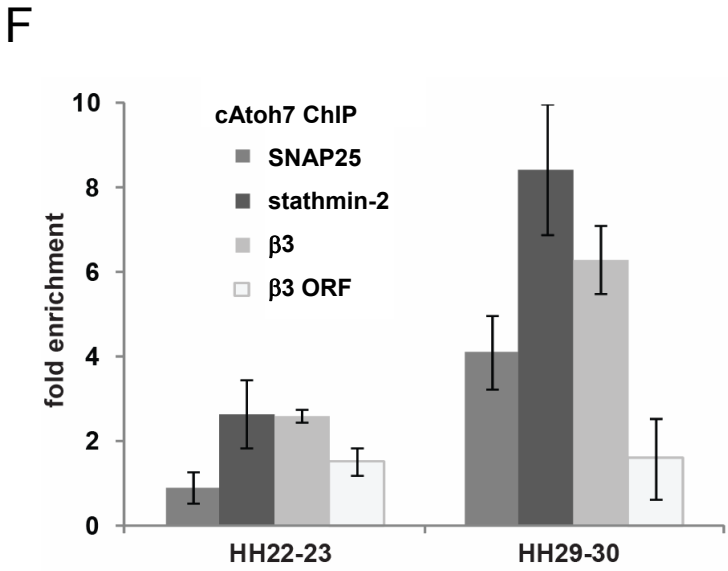
F
10
8
6
4
2
0
fold enrichment
cAtoh7 ChIP
SNAP25
stathmin-2
β3
β3 ORF
HH22-23
HH29-30

Figure S9

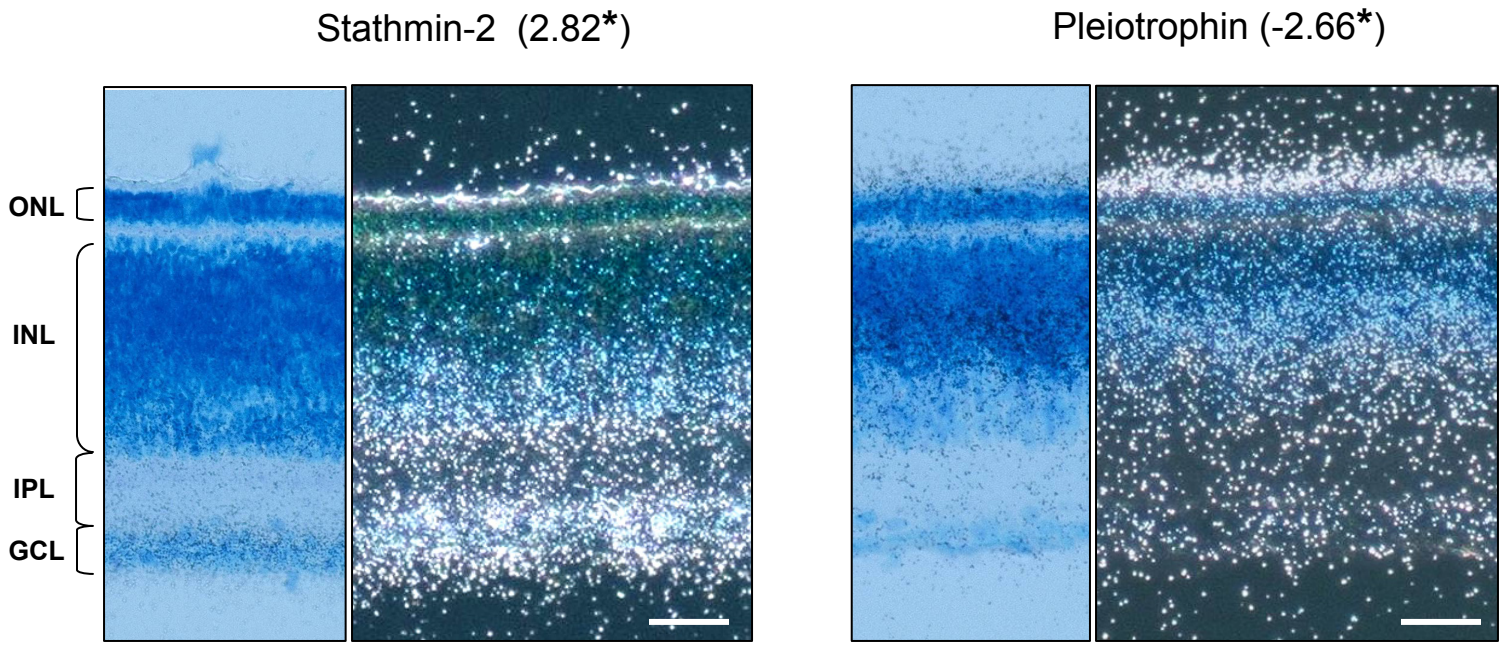

* **fold-increase in immunopanned RGCs (see Figure 6A)**